Managing Hazmat Emergency Logistics with Random Travel Time: A Distributionally Robust Approach

by

© Franklin C. Onwa

A thesis submitted to the
School of Graduate Studies
in partial fulfilment of the
requirements for the degree of
Master of Science

Faculty of Business Administration

Memorial University of Newfoundland

August 2024

St. John's Newfoundland and Labrador

Abstract

In the field of emergency logistics involving hazardous materials (hazmat), the optimization of emergency facility locations and risk mitigation is paramount. Prior research primarily focused on emergency planning with deterministic travel times. However, real-world emergency responses encounter diverse factors leading to uncertainties in travel duration. This study addresses the hazmat emergency facility location and allocation problem by considering stochastic emergency response times. The proposed distributionally robust optimization model aims to minimize emergency facility construction costs while concurrently mitigating potential system risk under the worst-case distribution of response time within an ambiguity set. Given limited distribution data derived from historical records, two methodologies are employed to convert this data into tractable ambiguity sets. Experimental assessments conducted using a hypothetical and a real-world case study in China showcase the superior efficacy and efficiency of the proposed approach. Furthermore, sensitivity analyses of parameters shed light on the various factors influencing the system, illustrating the interplay between cost minimization and risk mitigation objectives, and offering optimal solutions for different parameter configurations. These findings yield invaluable insights for decision-makers involved in hazmat emergency response operations.

Acknowledgements

I wish to express my heartfelt appreciation to Dr. Ginger Y. Ke, my supervisor, for her unwavering support, invaluable advice, and encouragement throughout my MSc. journey. Her wealth of knowledge has been immensely beneficial to my academic and research endeavors.

In addition to my supervisor, my appreciation is directed to Dr. David M. Tulett for his rich input, the Faculty of Business Administration, Mitacs and The Husky Centre, for the research funding.

I am grateful to my parents and siblings for their unwavering support throughout my educational journey, without which none of this would have been possible. I also extend my appreciation to my friends and colleagues, Anita, Reihaneh, Abed, Jacob, Jay, and many others, who have been a constant source of motivation.

Contents

List of Tables

List of Figures

Chapter 1

Introduction

Hazardous materials (hazmat) represent a critical product of modern industry, commerce, and daily life. These materials, while essential for various economic activities, pose substantial risks when accidents occur. Hazmat incidents, which include chemical spills, fires, transportation accidents, and industrial mishaps involving hazardous materials, can have severe consequences, including threats to human health, environmental degradation, and property damage. Consequently, regulatory bodies both nationally and internationally mandate proper handling, transportation, and disposal of hazmat to avert harm. Nevertheless, as the usage of hazmat continues to surge, so do hazmat incidents and associated risks. For instance, in 2020, the detonation of about 2,750 tonnes of stored ammonium nitrate caused a massive explosion at the Port of Beirut in Lebanon, resulting in at least 218 deaths, 7,000 injuries, and approximately 15 billion US Dollars in property damage (Cookman, 2020). Also, in

February 2023, a 38-car train derailment in Ohio led to widespread exposure to carcinogenic compounds, termed "an ecological and human health disaster" by experts (Rance, 2023). Recently, a hazmat cargo truck transporting anhydrous ammonia crashed in Illinois in September 2023, resulting in at least 5 deaths and the evacuation of approximately 490 Teutopolis residents around the 7,500-gallon spill (NYT, 2023). These instances, like many others worldwide, underscore the diversity of hazmat incidents occurring across industrial sites, transportation networks, and even residential areas.

Effective preparedness, mitigation, and response strategies are paramount in minimizing human suffering and loss during such disasters (Gao and Cao, 2020). Hence, emergency management necessitates the establishment of specialized facilities and the allocation of resources to address various aspects of the incident (Hamouda et al., 2004). These resources may include trained personnel, specialized equipment, decontamination facilities, and protective gear which play a pivotal role in ensuring efficient response during an incident. Consequently, various researchers have attempted to solve the hazmat emergency facility location problem, which addresses the spatial and resource allocation aspects of hazmat emergency management, with the goal of optimizing these processes for better preparedness and emergency response. Notably, the timely and effective response to hazmat incidents requires adequate emergency facilities that are reliable and strategically located to minimize response times and maximize the potential for successful outcomes (Ke, 2022).

Current guidelines for hazmat emergency response planning acknowledge the critical importance of well-placed hazmat teams (Hamouda et al., 2004), moreover, response time plays a crucial role in hazmat emergency response. The proactive intervention of an emergency response unit can significantly mitigate the consequences of a hazmat accident on the population and surrounding environment. For instance, Portland Fire and Rescue (2008) in their emergency response coverage standards, specified that any delay of one minute in defibrillation in an emergency could lead to a 10% reduction in survival rate. Moreover, their report emphasizes that hazmat response units can arrive at 90% of hazmat accidents within 18 minutes in urban areas while maintaining an acceptable level of response. It is crucial to note that any response delay beyond a certain defined threshold can significantly escalate the consequences of a hazmat incident.

However, in real-world scenarios, a recurring challenge in emergency response involves the variability associated with traveling times from an emergency facility to incident locations due to diverse factors such as weather and road conditions, lack of coordination, traffic congestion, and so on. Specifically, the uncertainty about the response timing, as well as its impacts, poses serious challenges to emergency preparedness and mitigation (Salman and Yücel, 2015). For instance, using historical fire data from 2010, Fig. 1.1 shows travel time statistics to six different places in Hefei, China (residence, business, dormitory, restaurant, warehouse, and plant). The data shown illustrates the diversity in fire rescue times, making it challenging to precisely

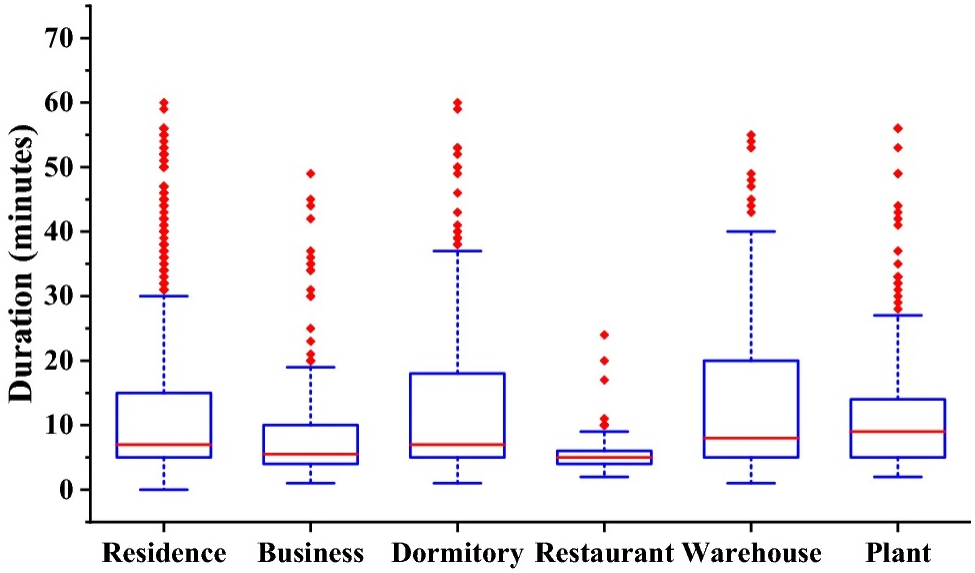

Figure 1.1: 1-year data of random fire response times among six different fire incidents (Ming et al., 2022)

forecast travel times beforehand (Ming et al., 2022). Furthermore, Chang et al. (2024) showed how unforeseen delays from road closures and road damages hinder access to emergency services and medical assistance in a disaster response, exacerbating human suffering and environmental impact (Chang et al., 2024).

Nevertheless, in addressing the hazmat emergency, researchers and practitioners have primarily overlooked the uncertainty of response time, assuming complete knowledge of travel factors and the precise nature of hazmat response in their models. These traditional models, while valuable in many optimization contexts, may be less suitable for hazmat emergency management due to the high level of uncertainty and variability associated with hazmat response. These variations, coupled with the unpredictability of human errors challenge the underlying assumption of

deterministic response time. Recognizing the limitations of this assumption in accounting for uncertainties, particularly in emergency response, this research opts for a Distributionally Robust Optimization (DRO) framework. While several reliable methodologies exist for handling uncertainties in the literature, precisely defining the variability and uncertainty present in response time estimation presents a challenge. This justifies our selection of DRO, due to its intricate nature of capturing and modeling the distribution of the variable parameters in uncertain scenarios. Hence, DRO represents an innovative approach that combines the elements of stochastic programming and robust optimization, offering a distinct advantage by leveraging partial knowledge of probability distribution information (Wang et al., 2022). The method is able to handle various uncertainties, encompassing challenges such as ambiguous probability distributions, limited availability of data, and complexities in accurately delineating random parameter distributions (Zhang et al., 2023a).

In this work, we apply a time-based risk approach considering uncertainty in travel time between emergency facilities and incident sites (response time) acknowledging the importance of timely response in emergency incidents. Like Taslimi et al. (2017), the response time is directly incorporated into the objective function, signifying that the expected risk within the system increases proportionally as response time increases. The significance of the present research lies in the following key contributions that distinguish it from existing literature. First, this work presents a single-level DRO model integrating chance constraints, capable of accommodating

the stochastic nature of hazmat emergency response by incorporating uncertainty in response times - a crucial situation often overlooked in previous studies. Thus, we strategically optimize the positioning of hazmat emergency facilities, acknowledging that the risk associated with hazmat transportation can be substantially reduced by thoughtfully situating emergency response units for their prompt response to incidents. Secondly, we employ a real-world hazmat emergency network as a case study, providing valuable insights for stakeholders involved in hazmat emergency logistics, aiding in the construction and management of a timely, high-performance response system.

The subsequent chapters in this thesis are organized as follows. Chapter 2 provides a comprehensive literature review of hazmat emergency logistics, hazmat emergency logistics with uncertainties, and DRO, setting the groundwork for our research. Chapter 3 presents the deterministic model of the hazmat emergency problem, encompassing the problem statement and the general assumptions. The DRO counterpart of the problem is presented in Chapter 4, as well as methodologies for solving the DRO model. Chapter 5 presents computational results from a hypothetical problem as well as a real-world transportation network for the proposed model. Chapter 6 summarizes our findings and outlines potential avenues for future research in hazmat emergency management.

Chapter 2

Literature Review

In this chapter, we present a thorough review focusing on critical areas within emergency logistics. Specifically, we delve into hazmat emergency logistics and emergency logistics in general, exploring the vital aspects of response planning, response optimization strategies, uncertainty management, and methodologies aimed at efficiently addressing hazmat incidents. Additionally, we highlight the emergence of Distributionally Robust Optimization (DRO) as a promising method for handling uncertainties in emergency logistics, providing insights into its applications and advancements in the field.

2.1 Hazmat Emergency Logistics

Hazmat emergency response planning and optimization has garnered significant attention in the literature, as it is crucial for ensuring effective and efficient response to incidents involving hazardous materials due to their catastrophic consequences. Appropriate resource allocation, rapid response times and the ability to deploy emergency response teams to the incident location are essential factors for ensuring a coordinated and efficient response. For this reason, important logistical planning, allocation, and optimization decisions must be made to address various aspects of the response (Hamouda et al., 2004). The first emergency logistics model was proposed by Saccomanno and Allen (1988), assuming the availability of rescue teams at all times and determining the optimal location of emergency facilities for responding to spill incidents. List (1993) followed with a multi-objective model to identify hazmat emergency response team sites for transportation-related incidents. Further, List and Turnquist (1998) formulated a route-siting model that integrated routing, flow assignment, and response team location decisions while Hamouda et al. (2004) introduced a risk-based optimization model to find the optimal hazmat response team location, ensuring response times fell within specified thresholds. Addressing arc-covering, Berman et al. (2007) developed a mathematical model for a highway network incorporating a pre-set coverage distance. Zografos and Androutsopoulos (2008) focused on location decisions optimizing response deployment for hazmat distribution routes based on evacuation time, risk, and cost. Maximizing service level,

Jiahong and Bin (2010) employed a maximal arc-covering model considering time and cost.

In real life scenarios, emergency response planning and optimization are complex tasks that involve dealing with various uncertainties inherent in emergency incidents, often characterized by limited historical data Li et al. (2011). These uncertainties pose challenges to decision-makers in the allocation of resources for disaster response. Scholars are increasingly focusing on addressing these uncertainties, such as uncertain transportation time (Paul and Wang, 2019), uncertain demand (Liu et al., 2019a; Boutilier and Chan, 2020), or uncertain allocation costs (Koca et al., 2021), to mention a few. In managing hazmat emergencies specifically, Ehsan et al. (2012) introduced a multi-objective hazmat emergency facility location model with uncertain demand characterized in a fuzzy random environment. Also, Xu et al. (2013) solved a bi-level programming model to address emergency response under a complex fuzzy risk environment. Xin et al. (2013) presented a robust optimization model for a hazardous materials transportation network design problem with uncertain edge risk while Berglund and Kwon (2014) introduced a robust hazmat facility location problem, taking into account the carrier's routing decisions under uncertain shipments and arcs. Sun et al. (2015), acknowledging risk uncertainty on network links, incorporated worst-case risk measures with an uncertainty budget in a robust optimization model for flexible decision-making. Ardjmand et al. (2015) utilized random numbers from a predefined interval to generate different scenarios for

transportation uncertainty, attributing equal probability to each scenario. In their study, Taslimi et al. (2017) explored robust scenario-based planning in a bi-level risk modeling problem that incorporated average response time, meanwhile Zhao and Ke (2019) in their study focus on optimizing emergency logistics in hazmat incidents through a novel two-level game theoretic model, which addresses the complexities of multi-quality coverages in facility location and allocation. Later, Vaezi et al. (2021) applied a two-stage stochastic programming model for response facility location and allocation of equipment packages in the field of railway hazmat emergency. Ke (2022) further examined facility and link disruptions within an emergency logistics framework for hazmat using a two-stage robust methodology. Following Vaezi et al. (2021) in response to railroad accidents, Wang et al. (2023b) proposed a rescue emergency facility location model based on an ellipsoidal robust framework, incorporating uncertain demand, service, and safety parameters. Recently, Ke and Bookbinder (2023) presented a bi-objective robust model for resilient emergency logistics infrastructure, incorporating uncertainties in demand and the potential unavailability of specific links.

2.2 Emergency Logistics under Uncertainties

In the broad field of emergency logistics amidst uncertainties, researchers have formulated different optimization models to address the issue of unpredictability. Three methods have been extensively utilized in the literature as follows; Stochastic Pro-

gramming, Fuzzy Methods and Robust Optimization.

Stochastic programming (SP) incorporates stochastic elements to make decisions under uncertainty, treating uncertain parameters as random variables with known distributions (Noyan, 2012). Rennemo et al. (2014) introduced a three-stage mixed-integer stochastic programming model with the purpose of planning the location and distribution of facilities encompassing unpredictable variables such as the availability of transport vehicles, the state of the infrastructure, and the demand from potential beneficiaries. Afterwards, a scenario-based stochastic mixed-integer non-linear program (MINLP) model was developed by An et al. (2015) to solve an integrated facility location problem. This study takes into account the potential consequences of facility outages, en-route traffic jams, and in-facility queuing delays. Wang et al. (2021a) introduced a preparedness-response model in two stages, employing scenario-based stochastic programming to optimize integrated facility pre-positioning and real-time emergency response. Ghelichi et al. (2022) employed stochastic optimization for the delivery of aid parcels to disaster-stricken regions using drones in uncertain demand locations, aiming to minimize overall disutility or cost. On the other hand, Sanada and Ishigaki (2023) accounted for unpredictability related to demand, road networks, and processing status of building materials through a stochastic programming approach considering finite scenarios. Dukkanci et al. (2023) considered uncertainties in demand fluctuations and road networks post-earthquake, formulating a relief distribution problem employing drones under uncertainty. This study presented formu-

lations for a two-stage stochastic programming problem.

Fuzzy methods have also been widely adopted in emergency logistics management and aim to handle uncertainties using fuzzy logic or fuzzy numbers. Bababeik et al. (2018) applied a fuzzy logic technique along with the augmented e-constraint method to solve a bi-level railway emergency facility location and allocation problem. Ren and Tan (2022) proposed a collaborative optimization approach for locating and allocating emergency distribution centers to minimize rescue time and maximize the rate of demand satisfaction. Taking into account uncertainties, a triangular fuzzy number method is adopted to estimate the emergency material demand and solved using a plant growth simulation algorithm. Chobar et al. (2022) investigated reverse logistics planning in earthquake scenarios, accounting for uncertainties through fuzzy methods in a multi-objective problem. Li (2023) utilized interval numbers to represent uncertain emergency material demands and formulated a location-based optimization model, converting interval uncertainty into specific values to address dual objectives of rescue cost and time. Finally, Wan et al. (2023) developed a multi-period dynamic emergency material distribution model using fuzzy numbers to depict uncertain demands and transportation times, solved by a hybrid multi-objective algorithm.

Robust optimization (RO) restricts uncertain parameters to predefined sets, and aims to address uncertainties in emergency logistics planning by creating resilient solutions (Baron et al., 2011; Paul and Wang, 2019). Liu et al. (2019b) developed an iterative ϵ–constraint-based model to maximize predicted survivals and minimize

total operational expenses in order to optimize the allocation plan for temporary medical services. They also presented an alternative robust optimization model. Shu et al. (2021) suggested a nonlinear mixed-integer programming model that optimises choices about the placement of facilities and the prepositioning of relief supplies while ensuring robustness against demand uncertainties. Notably, Aliakbari et al. (2022) introduced a scenario-based robust optimization model for relief logistics planning that encompasses pre- and post-disaster measures, addressing uncertain demand and travel times. Akbari et al. (2022) presented a robust scenario-based optimization model for various potential disaster scenarios aimed at minimizing unmet demands and transportation expenses for relief vehicles within affected regions. In the same vein, Sun et al. (2022) presented a novel scenario-based robust bi-objective optimization model integrating casualty transportation, facility location, and relief commodity allocation while accounting for interruption risks, while Eshghi et al. (2022) formulated a robust location-allocation planning framework for emergency relief, incorporating various logistics factors and uncertainties into a multi-objective model. Recently, Zhang et al. (2023b) constructed a capacitated, multi-period, multi-echelon deployment of facilities and resource allocation, aiming to bolster decision reliability. To counteract the overly conservative nature of robust solutions amid an epidemic's progression, an adjustment strategy for uncertainty budgets was proposed. Du et al. (2023) developed a multi-stage mixed-integer linear programming model focusing on integrated strategies encompassing primary and secondary disaster management

employing a multi-stage robust framework to address uncertainties.

Other methods have also been employed in the emergency literature. To solve the problem of the location of emergency response facilities under different uncertainties, Zhang et al. (2017) applied uncertainty programming in their model and distinguished its application from fuzzy set theory. In the same vein, Li et al. (2017) utilized uncertainty theory to create robust solutions for distributing medical supplies during emergencies with uncertainties in demand and transportation duration. Ding et al. (2022) introduced an emergency material scheduling model using grey interval numbers, optimized through a genetic algorithm for robust decision-making in emergency relief. Furthermore, for a thorough review of the literature in emergency logistics, we direct readers to Wang et al. (2021b) and Kundu et al. (2022), which highlight the impact, topics, and methodological reach of the journal in the area of emergency facility location and general emergency logistics management respectively.

2.3 DRO in emergency logistics

From the literature, we see that different optimization techniques have been extensively explored in the field of emergency logistics to find optimal solutions for problems involving uncertain data. While SP overlooks the limitations in obtaining the exact distributions for variables due to limited data, RO introduces overconservatism, failing to fully utilize the potential information derivable from historical data (Wang et al., 2022).

Distributionally Robust Optimization (DRO) offers an alternative paradigm that combines elements of both stochastic programming and robust optimization, aiming to overcome their deficiencies by utilizing only partial information about the distribution. This approach has gained attention, especially during the past decade, offering a more flexible way to handle uncertainty, including but not limited to ambiguity in probability distributions, limited data availability, and challenges in accurately characterizing the distribution of random parameters (Zhang et al., 2023a). This technique has been effectively applied to various research areas, including traffic planning and management (Sun et al., 2014), scheduling (Xia et al., 2023), emergency response dispatch (Yang et al., 2019; Zhang et al., 2023c), inter-modal hinterland transportation (Dai and Yang, 2020), energy management (Zhao et al., 2020; Yin and Zhao, 2022) to name a few, but herein we focus our discussions on emergency related applications.

Liu et al. (2019a) proposed a DRO model for optimizing a hub location problem in an emergency medical service (EMS) system by minimizing the expected total cost under uncertain demands. The model introduced joint chance constraints and characterized the expected total cost by moment uncertainty based on a data-driven approach. In another study, Zhang et al. (2020) presented a DRO model with mean absolute semi-deviation for a humanitarian relief network design problem involving resource reallocation after an uncertain disaster environment. With the successes recorded in DRO, Ming et al. (2022) explored a DRO model for optimizing the loca-

tion of fire stations, the number of fire trucks, and demand assignment for long-term planning in an emergency fire service system. In the same vein, Zhang et al. (2022) addressed the challenge of designing an emergency rescue network in response to uncertainties after disasters. They employ the mean absolute deviation (MAD) for constructing the ambiguity set and introduce a linear decision rule to reformulate the complex model. Following that, Shehadeh and Tucker (2022) proposed and analyzed a disaster relief problem with a two-stage stochastic programming (SP) and DRO model, assuming known and unknown (ambiguous) uncertainty distributions, while Wang et al. (2022) introduced a modified version of the p-center problem (PCP) for the location of high-speed railway emergency rescue stations under uncertain travel time, and proposed a safe and tractable approximation method to transform the original DRO model into mixed-integer second-order cone programs. Wang et al. (2023a) introduced a comprehensive model integrating facility location, inventory management, and multi-commodity network flow, considering partially known probability distribution details regarding supply, demand, and road link capacity.

2.4 Literature Gap and Our Contribution

In recent years, the literature has seen a growing body of research dedicated to various aspects of hazmat transportation. Hazmat risk assessment for instance has seen significant evolution, progressing from models like the Traditional Risk (TR) to more advanced approaches for quantifying and managing risks (Ke et al., 2024).

However, despite their advancements, a significant gap exists in capturing the impact of random response times in emergency response, particularly as a result of weather, road conditions, lack of coordination, traffic congestion, and other factors within a transportation network. Also, existing studies in the domain of emergency logistics lack dedicated methodologies tailored for hazmat emergency logistics. They predominantly rely on Stochastic and Robust Optimization techniques, which tend to over-constrain uncertainties and not fully leverage historical data.

Recognizing this gap in research considering emergency response effectiveness in risk assessment, we integrate a measure of uncertain response time from hazmat response units to the incident location. This inclusion better reflects the stochastic behavior of risk, emphasizing the impact of faster response times in minimizing overall risk. We recognize that precise information cannot be known, thus to overcome the limitations of Stochastic and Robust Optimization techniques, we assume that only partial knowledge of the distribution of response time is known, and propose an emergency DRO model that minimizes the risk of hazmat incidents and facility location costs concurrently. To the best of our knowledge, this work represents the first time that the benefits of DRO methodology in handling real-world unpredictability are extended to hazmat emergency literature, aiming to improve planning efficiency and robustness in hazmat incident response. Finally, we demonstrate that the proposed DRO model is efficient, as we test our model against a hypothetical case study and also apply it to a real transportation network in China to evaluate their

effectiveness in locating emergency facilities and assessing risk. We also compare the computational efficiency and accuracy of the proposed solution methods.

Chapter 3

Deterministic Model

3.1 Problem Statement

We address the location and allocation of emergency facilities and emergency units for hazmat emergencies involving numerous potential emergency facilities and multiple incident sites, illustrated through a bipartite graph structure as shown in Fig. 3.1. Suppose the road network $\mathcal{N}(\mathcal{V}, \mathcal{E})$ is composed of vertex set $\mathcal{V}$ and edge set $\mathcal{E}$. We have $\mathcal{V} = \mathcal{I} \cup \mathcal{J}$, where $\mathcal{I}$ and $\mathcal{J}$ represent the sets of emergency facility locations and incident sites respectively. Multiple hazmat types $k \in \mathcal{K}$, where $\mathcal{K}$ is the complete set of hazmat types, may be stored at each incident site $j \in \mathcal{J}$, and may exhibit distinct spill probabilities and consequences following an incident. The emergency requirement of hazmat k at incident site j during an incident is denoted as W_{jk}, and the emergency facilities must satisfy the system emergency requirement. The

allocation of emergency units x_{ijk} to incident sites depends on their availability, hence each emergency facility i needs to maintain different types of emergency units to handle incidents. Each emergency facility incurs a setup cost FC_i and has a capacity CF_i, determining the maximum emergency units it can handle. Meanwhile, a variable cost VC_{ik} exists for maintaining each emergency unit of type k at facility i. Notably, each emergency unit responds specifically to incidents caused by a single type of hazmat. Given an available facility construction budget B and the set of potential facility locations, we address the hazmat emergency location problem aiming to locate emergency facilities and allocate emergency units to incident sites. The objective is to minimize the total system risk while also minimizing overall costs, encompassing both construction and maintenance expenses.

3.2 Response Time

This paper adopts the traditional risk definition proposed by Alp (1995). We define the potential risk at incident site j caused by Hazmat k as follows:

$$E_{jk} = PR_j \cdot RE_k \cdot PO_{jk} \tag{3.1}$$

Here, PR_j represents the incident rate at incident site j, RE_k denotes the release rate of Hazmat k if an incident occurs, and PO_{jk} quantifies the population exposed due to an incident involving Hazmat k at incident site j.

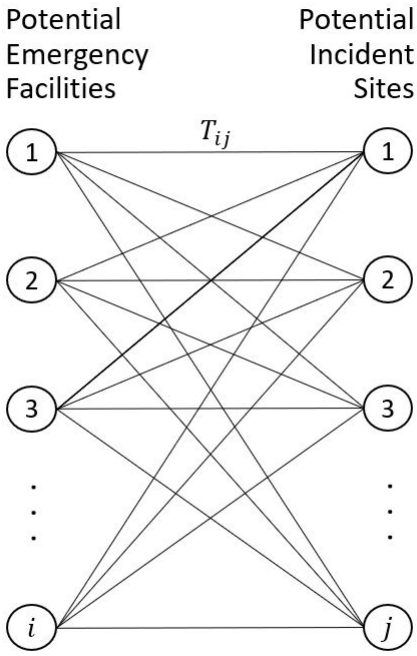

Figure 3.1: Bipartite network structure

A guide for evaluating emergency response requirements in hazmat incidents (Board, 2011) highlighted a direct relationship between response time and risk. Taking this into consideration, we now express the overall system risk as follows.

$$\sum_{i\in\mathcal{I}}\sum_{j\in\mathcal{J}}\sum_{k\in\mathcal{K}} T_{ij}E_{jk}x_{ijk} \tag{3.2}$$

Previously, Zhao and Ke (2019), Ke (2022), Ke and Bookbinder (2023) connected the time with risk through a Response Time Factor (RTF). Differing from this, we

incorporate the response time directly into the objective function, signifying that the expected risk within the system increases proportionally as response response time increases.

Equation (3.2) captures the total system risk associated with the response time T_{ij} for which an emergency unit travels from one facility i to an incident location j. It calculates the overall system risk incurred as the time changes for a hazmat emergency response. Moreover, the degree of uncertainty associated with the response time due to weather, road conditions, lack of coordination, traffic congestion, and other factors is an important challenge in the process of hazmat emergency response (Zhang et al., 2023c). Taking these factors into consideration, this research applies a time-based risk approach considering uncertainties in travel time between facility locations and incident sites. For each pair of emergency facility i and incident site j, T_{ij} represents the response time from facility i to site j. Our linear relationship between response time and Hazmat risk accounts for the time-sensitive nature of emergency response since faster responses have the potential to reduce the severity of emergency consequences.

3.3 Assumptions and Notation

3.3.1 Assumptions

The following assumptions are made in this work. First, due to the urgency of responses, this study operates under the foundational presumption that all available links for emergency response within the network comply with government regulations. This critical adherence ensures that these links are reliably accessible by hazmat emergency units, aligning with the need for swift and timely responses in hazmat emergencies.

Second, it is fundamental to this study's framework that each incident caused by hazmat type k necessitates a tailored response strategy. Accordingly, the assumption is made that each incident caused by hazmat type k can only be responded to by the corresponding emergency unit designated for handling the identified hazard type. This assumption emphasizes the specialization and targeted expertise required in hazmat emergency response scenarios.

Also, considering the complex network of emergency responses, this model adopts the assumption that the shortest path between any given facility $i \in \mathcal{I}$ and destination $j \in \mathcal{J}$ serves as the response path.

Fourth, an integral aspect incorporated into the model involves the capacitated nature of emergency facilities. It is assumed that these facilities possess finite capacity limits, allowing for only a predetermined number of emergency units to be

operational at any given time. This assumption underscores the necessity for resource management and strategic allocation, considering the capacity limitations of real-world facilities.

Lastly, acknowledging the real-world constraints faced by decision-makers, this model considers budgetary limitations concerning the construction of emergency facilities. This assumption mirrors the practical challenges encountered by authorities and decision-makers, emphasizing the need for judicious financial planning and allocation in establishing effective emergency response infrastructure.

3.3.2 Notation

The notation for parameters and decision variables used throughout this chapter are presented in Table 3.1.

3.4 Deterministic model

We consider that hazmat emergency facilities need to be located to respond to Hazmat emergencies at incident sites. We have a set of candidate facility locations, and we want to determine the optimal number and locations for emergency facilities. We present the cost formulations thus.

$$\text{Cost of facility} = \sum_{i \in \mathcal{I}} FC_i y_i$$

Table 3.1: Mathematical notation

Sets	
$\mathcal{I}$	Set of candidate emergency facility locations, indexed by i.
$\mathcal{J}$	Set of incident sites, indexed by j.
$\mathcal{K}$	Set of Hazmat types, indexed by k.
Parameters	
θ	Maximum allowable time for hazmat emergency response.
γ	Risk coefficient evaluating the importance or cost of risk.
FC_i	Fixed cost of locating an emergency facility at node i.
VC_{ik}	Variable cost of maintaining one emergency unit for k at facility i.
CF_i	Capacity of facility i.
W_{jk}	Emergency requirement for Hazmat type k at site j.
E_{jk}	Potential risk at incident site j caused by Hazmat k.
T_{ij}	Response time from facility i to site j.
B	Available budget for facility construction.
M	A large positive integer.
Variables	
y_i	1 if emergency facility is located at facility i; 0 otherwise.
q_{ik}	Number of emergency units for hazmat type k pre-positioned at facility i.
x_{ijk}	Number of emergency units dispatched from facility i to incident site j responding to hazmat type k.
l_{ijk}	1 if link from facility i to site j is used for emergency response for hazmat type k; 0 otherwise.

$$\text{Cost of maintaining supplies} = \sum_{i\in\mathcal{I}}\sum_{k\in\mathcal{K}} VC_{ik}q_{ik}$$

Next, we present the deterministic model of the problem as follows.

[**DET**]

$$\min \sum_{i\in\mathcal{I}} FC_i y_i + \sum_{i\in\mathcal{I}}\sum_{k\in\mathcal{K}} VC_{ik}q_{ik} + \gamma \cdot \sum_{i\in\mathcal{I}}\sum_{j\in\mathcal{J}}\sum_{k\in\mathcal{K}} T_{ij}E_{jk}x_{ijk} \tag{3.3}$$

s.t.

$$\sum_{k\in\mathcal{K}} q_{ik} \le CF_i y_i, \qquad \forall i \in \mathcal{I} \tag{3.4}$$

$$\sum_{j\in\mathcal{J}} x_{ijk} \le q_{ik}, \qquad \forall i \in \mathcal{I}, \forall k \in \mathcal{K} \tag{3.5}$$

$$\sum_{i\in\mathcal{I}} x_{ijk} \ge W_{jk}, \qquad \forall j \in \mathcal{J}, \forall k \in \mathcal{K} \tag{3.6}$$

$$T_{ij}l_{ijk} \le \theta, \qquad \forall i \in \mathcal{I}, \forall j \in \mathcal{J}, \forall k \in \mathcal{K} \tag{3.7}$$

$$l_{ijk} \le x_{ijk}, \qquad \forall i \in \mathcal{I}, \forall j \in \mathcal{J}, \forall k \in \mathcal{K} \tag{3.8}$$

$$x_{ijk} \le Ml_{ijk}, \qquad \forall i \in \mathcal{I}, \forall j \in \mathcal{J}, \forall k \in \mathcal{K} \tag{3.9}$$

$$\sum_{i\in\mathcal{I}} FC_i y_i \le B \tag{3.10}$$

$$y_i \in \{0,1\}, \qquad \forall i \in \mathcal{I} \tag{3.11}$$

$$l_{ijk} \in \{0,1\}, \qquad \forall i \in \mathcal{I}, \forall j \in \mathcal{J}, \forall k \in \mathcal{K} \tag{3.12}$$

$$q_{ik} \ge 0, \text{ integer}, \qquad \forall i \in \mathcal{I}, \forall k \in \mathcal{K} \tag{3.13}$$

$$x_{ijk} \geq 0, \text{ integer}, \qquad \forall i \in \mathcal{I}, \forall j \in \mathcal{J}, \forall k \in \mathcal{K} \tag{3.14}$$

The objective function (3.3) consists of multiple components that collectively capture the cost and risk objectives of the hazmat emergency problem. In summary, the objective function aims to minimize the costs associated with facility location, maintenance, and total system risk. The coefficient γ acts as a weighting factor to normalize and integrate the cost and risk into a single objective function, allowing the decision maker to control the trade-off between minimizing costs and minimizing risks. The normalization ensures that these differing components can be balanced within the optimization model, which is a common practice in multi-objective optimization, in line with existing literature. The choice of γ is guided by sensitivity analysis or empirical data, provided in Chapter 5. Hence, a higher value of γ will emphasize the importance of risk reduction in the optimization and vise versa. Constraint (3.4) ensures that the total quantity of emergency relief groups pre-positioned at a facility does not exceed its capacity if the facility is opened. Constraint (3.5) imposes a limit on the number of emergency units dispatched from a facility based on the pre-positioned emergency units. Constraint (3.6) requires that the total number of dispatched emergency units serving an incident site for hazmat type k should meet or exceed the emergency requirement. Constraint (3.7) restricts the response time for any emergency response to be within a given threshold. Constraints (3.8) and (3.9) link binary variable l_{ijk} with continuous variable x_{ijk}, reflecting the relationship be-

tween link usage and dispatched emergency units. Constraint (3.10) limits the total cost associated with facility construction to a maximum budget. Constraint (3.11) and (3.12 specifies the binary decision variables for facility location and link usage respectively. Constraint (3.13) sets the non-negativity and integer requirements for variables related to the emergency relief groups. Constraint (3.14) specifies the characteristics of the variable representing the amount of emergency requirement satisfied by facilities.

Chapter 4

Distributionally Robust Optimization Model and Solution

The parameter θ in our deterministic model plays a crucial role in limiting the response time T_{ij} for hazmat emergency units from emergency facilities to incident sites. While in a controlled setting, a strict pre-determined response time might seem feasible, nevertheless, real-world scenarios present uncertainties due to uncontrollable factors like weather, road conditions, traffic, and vehicle specifications, making the use of deterministic response times unrealistic. These unpredictable factors could potentially extend the response time beyond the specified threshold. Consequently, by adopting a flexible approach and treating T_{ij} as a parameter subject to variation, we acknowledge the practical constraints faced during hazmat emergency response. This necessity for flexibility and adaptability leads us to employ DRO

techniques to address uncertainties surrounding T_{ij}, ensuring a more resilient and effective emergency response strategy that considers the inherent unpredictabilities in hazmat emergency scenarios. Thus, we present a DRO variant addressing this uncertainty.

4.1 Formulation of the DRO

Considering the presence of incomplete information regarding the actual probability distributions of the system response times as introduced above, we adopt the assumption that the unpredictable response time is influenced by random deviations resulting from incomplete historical data (Wang et al., 2022; Yin et al., 2019):

$$T_{ij} = \bar{T}_{ij} + \zeta_{ij}\hat{T}_{ij}, \quad \forall i \in \mathcal{I}, \forall j \in \mathcal{J}$$

In this context, $\bar{T}_{ij}$ represents the expected or average value, $\hat{T}_{ij}$ signifies the normal deviation of the uncertain variable, and ζ_{ij} is a random variable with limited information regarding its probability distribution, otherwise the perturbation variable. With these specified uncertain perturbation parameters, we modify constraint (3.7) to incorporate this response time uncertainty in the system as follows

$$(\bar{T}_{ij} + \zeta_{ij}\hat{T}_{ij})l_{ijk} \leq \theta. \tag{4.1}$$

Furthermore, for $\epsilon \in (0,1)$ representing a pre-determined small tolerance level, the following chance constraint satisfies constraints (4.1) when the perturbation variable ζ_{ij} is random and has a probability distribution P:

$$\text{Prob}_{\zeta \sim P}\left\{\bar{T}_{ij} l_{ijk} + \zeta_{ij} \hat{T}_{ij} l_{ijk} \leq \theta\right\} \geq 1 - \epsilon \tag{4.2}$$

The choice of ϵ depends on the desired balance between robustness and optimality by decision maker. Smaller ϵ values lead to more conservative solutions, ensuring robustness under uncertainty, while larger values allow for more aggressive optimization with potentially lower costs. Sensitivity analysis or empirical data should guide the selection of ϵ, which we have provided in Chapter 5.

We utilize $\text{Prob}_{\zeta \sim P}(\{\cdot\})$ to indicate the likelihood of the event within the parentheses under the probability distribution P. However, accurately determining the probability information about the random response time from one facility location to a Hazmat emergency site is challenging due to the previously highlighted factors such as weather conditions, road state, traffic congestion, emergency vehicle type, speed, etc. As a result, when the probability distribution P of ζ_{ij} belongs to a given general ambiguity set $\mathcal{P}$, we outline the ambiguous chance constraints as follows:

$$\inf_{P \in \mathcal{P}} \text{Prob}_{\zeta \sim P}\left\{\bar{T}_{ij} l_{ijk} + \zeta_{ij} \hat{T}_{ij} l_{ijk} \leq \theta\right\} \geq 1 - \epsilon \tag{4.3}$$

In Equation (4.3), we employ $\inf_{P \in \mathcal{P}}\{\cdot\}$ to represent the most challenging or worst-

case situation, which illustrates robustness. It is crucial to emphasize that we possess only partial information about the probability distribution in advance, specifically regarding its support, mean, and variance.

Based on the chance constraint and the terminology introduced in the previous sections, we present the following DRO model for the given problem:

[**DRO**]

$$\min \sum_{i\in\mathcal{I}} FC_i y_i + \sum_{i\in\mathcal{I}}\sum_{k\in\mathcal{K}} VC_{ik} q_{ik} + \gamma \cdot \sum_{i\in\mathcal{I}}\sum_{j\in\mathcal{J}}\sum_{k\in\mathcal{K}} (\bar{T}_{ij} + \zeta_{ij}\hat{T}_{ij}) E_{jk} x_{ijk} \tag{4.4}$$

S.t.

$$\sum_{k\in\mathcal{K}} q_{ik} \leq CF_i y_i, \qquad \forall i \in \mathcal{I} \tag{4.5}$$

$$\sum_{j\in\mathcal{J}} x_{ijk} \leq q_{ik}, \qquad \forall i \in \mathcal{I}, \forall k \in \mathcal{K} \tag{4.6}$$

$$\sum_{i\in\mathcal{I}} x_{ijk} \geq W_{jk}, \qquad \forall j \in \mathcal{J}, \forall k \in \mathcal{K} \tag{4.7}$$

$$l_{ijk} \leq x_{ijk}, \qquad \forall i \in \mathcal{I}, \forall j \in \mathcal{J}, \forall k \in \mathcal{K} \tag{4.8}$$

$$x_{ijk} \leq M l_{ijk}, \qquad \forall i \in \mathcal{I}, \forall j \in \mathcal{J}, \forall k \in \mathcal{K} \tag{4.9}$$

$$\sum_{i\in\mathcal{I}} FC_i y_i \leq B \tag{4.10}$$

$$\inf_{P\in\mathcal{P}} \text{Prob}_{\zeta\sim P}\left\{\bar{T}_{ij} l_{ijk} + \zeta_{ij}\hat{T}_{ij} l_{ijk} \leq \theta\right\} \geq 1-\epsilon, \qquad \forall i,j \in \mathcal{V}, \forall k \in \mathcal{K} \tag{4.11}$$

$$y_i \in \{0,1\}, \qquad \forall i \in \mathcal{I} \tag{4.12}$$

$$l_{ijk} \in \{0,1\}, \qquad \forall i \in \mathcal{I}, \forall j \in \mathcal{J}, \forall k \in \mathcal{K} \quad (4.13)$$

$$q_{ik} \geq 0, \text{ integer}, \qquad \forall i \in \mathcal{I}, \forall k \in \mathcal{K} \quad (4.14)$$

$$x_{ijk} \geq 0, \text{ integer}, \qquad \forall i \in \mathcal{I}, \forall j \in \mathcal{J}, \forall k \in \mathcal{K} \quad (4.15)$$

4.2 Solution Procedure

The performance of DRO solutions significantly depends on the construction of the ambiguity set, which should contain the true distribution with high confidence while avoiding over-conservativeness (Zhang et al., 2022). The DRO approach poses a hard optimization problem that is computationally intractable, since the ambiguous chance constraints cannot be turned into an equivalent deterministic model. To help with this, constructed ambiguity sets facilitate the transition from the original model to a tractable form (Zhang et al., 2023a). So far, different works have studied diverse aspects of uncertainty and offer unique solutions to the respective problems, such as considering both distributional forms and moment information, tractable approximation, Wasserstein distance-based ambiguity set, and many more (Delage and Ye, 2010; Xia et al., 2023). For the suggested model, we approach the problem using two computable forms of ambiguity sets, consisting of possible distributions of the uncertain response time and convert the original model into manageable counterparts while working within predefined bounded and Gaussian perturbation ambiguous sets as originally proposed by Ben-Tal et al. (2009); Yin et al. (2019).

4.2.1 Solution under bounded zero-mean perturbations

This section focuses on creating a tractable convex approximation that remains safe under bounded perturbations with zero mean. This involves approximating within the feasible area, essentially remaining within the initial feasible region (Wang et al., 2022). The objective here is to construct a tractable convex approximation for the uncertain chance constraint. To achieve this goal, the assumptions listed below about the ambiguity set $\mathcal{P}$ are adopted.

Assumptions. $\{\zeta_{ij}\}$ are independent variables; support of the random variables $|\zeta_{ij}| \leq 1$; mean of the random variables $\mathbf{M}[\zeta_{ij}] = 0$ (Yin et al., 2019).

Under these aforementioned assumptions, establishing a safe convex approximation for an uncertain chance constraint like our problem is facilitated. We proceed to present a lemma that proves useful pertaining to the tractable reformulation of the ambiguous chance constraint.

Lemma 4.2.1. Let $\hat{T}_{ij}$ be deterministic coefficients and $\zeta_{ij} = [-1, 1]$ be independent random variables with zero mean. Then for any auxiliary variable $\Psi \geq 0$, it holds that

$$\text{Prob}\left\{\zeta_{ij}\hat{T}_{ij}l_{ijk} > \Psi\sqrt{(\hat{T}_{ij}l_{ijk})^2}\right\} \leq \exp\{-\Psi^2/2\}, \forall i \in \mathcal{I} \tag{4.16}$$

Proof. Suppose we define a variable Z_{ij}, where

$$Z_{ij} = \frac{\hat{T}_{ij}l_{ijk}}{\sqrt{(\hat{T}_{ij}l_{ijk})^2}}$$

By transforming the above formula, through normalization, we have

$$Z_{ij}^2 = 1.$$

We proceed to demonstrate that

$$\text{Prob}\left\{Z_{ij}\zeta_{ij} > \Psi\right\} \leq \exp\{-\Psi^2/2\}.$$

The goal is to relate the probability to an expectation using the exponential function. We start with the Chebyshev's inequality and rewrite the probability in terms of an exponential

$$\text{Prob}\left\{Z_{ij}\zeta_{ij} > \Psi\right\}$$

$$= \text{Prob}\left\{\exp\left\{Z_{ij}\zeta_{ij}\Psi\right\} > \exp\{\Psi^2\}\right\}.$$

Using the definition of expectation, the exponential of the random variables is less than or equal to the expectation of the exponential

$$\leq \exp\{-\Psi^2\}\mathbb{E}\left[\exp\left\{Z_{ij}\zeta_{ij}\Psi\right\}\right].$$

Since ζ_{ij} are independent, the expectation of the product of exponential becomes a product of expectations. Hence

$$\exp\{-\Psi^2\}\mathbb{E}\left[\exp\left\{Z_{ij}\zeta_{ij}\Psi\right\}\right]$$

$$= \exp\{-\Psi^2\}\mathbb{E}\left[\exp\left\{Z_{ij}\zeta_{ij}\Psi\right\}\right].$$

Due to the symmetry of the distribution of $\zeta_{ij} \in [-1, 1]$, considering the Taylor series expansion for the expectation of the exponential term, it simplifies to a known expression as

$$\mathbb{E}\left[\exp\left\{Z_{ij}\zeta_{ij}\Psi\right\}\right] = \sum_{l=0}^{\infty}\left[\frac{(Z_{ij}\Psi)^{2l}}{(2l)!}\right] \leq \exp\left\{Z_{ij}^2\Psi^2/2\right\}.$$

Finally, using the Chernoff bound and manipulating the expectation of the exponential term, we establish the inequality for the probability in terms of the expectation. Also, since $Z_{ij}^2 = 1$, we can prove that

$$\text{Prob}\left\{Z_{ij}\zeta_{ij} > \Psi\right\} \leq \exp\{-\Psi^2\}\exp\{\Psi^2/2\} = \exp\{-\Psi^2/2\}.$$

The proof is complete. □

Theorem 4.2.1. If random variable $\hat{T}_{ij}$ fulfills the criteria outlined in Lemma 4.2.1, the robust counterpart of the uncertain inequality

$$\bar{T}_{ij}l_{ijk} + \zeta_{ij}\hat{T}_{ij}l_{ijk} \leq \theta$$

can be transformed into the form

$$\bar{T}_{ij}l_{ijk} + \Psi\sqrt{(\hat{T}_{ij}l_{ijk})^2} \leq \theta \tag{4.17}$$

where

$$\Psi > \sqrt{2\ln(1/\epsilon)} \tag{4.18}$$

Proof. We will prove that Equations (4.17) and (4.18) are the sufficiency conditions of Equation (4.11) under the assumptions made for the ambiguity sets $\mathcal{P}$. Given the ambiguous chance constraint (4.11), we seek to to transform the inequality into an equivalent form. Rearranging constraint (4.11), we express the condition where the probability of the sum exceeding θ is less than ϵ as

$$\text{Prob}\left\{\bar{T}_{ij}l_{ijk} + \zeta_{ij}\hat{T}_{ij}l_{ijk} > \theta\right\} < \epsilon. \tag{4.19}$$

Hereafter, we need to prove that, for a given solution, if Eq. (4.17) and (4.18) hold, it must have Eq. (4.19) with at least prob $1 - \exp\{-\Psi^2/2\}$. Given that

$$\bar{T}_{ij}l_{ijk} + \Psi\sqrt{(\hat{T}_{ij}l_{ijk})^2} \leq \theta < \bar{T}_{ij}l_{ijk} + \zeta_{ij}\hat{T}_{ij}l_{ijk}$$

according to Lemma 1, it has been proven that if Equation (4.17) holds, the proba-

bility of an expression being greater than θ is less than ϵ, hence we can obtain

$$\begin{aligned}
\text{Prob}\left\{\bar{T}_{ij}l_{ijk} + \zeta_{ij}\hat{T}_{ij}l_{ijk} > \theta\right\} &\leq \text{Prob}\left\{\bar{T}_{ij}l_{ijk} + \zeta_{ij}\hat{T}_{ij}l_{ijk} > \bar{T}_{ij}l_{ijk} + \Psi\sqrt{(\hat{T}_{ij}l_{ijk})^2}\right\} \\
&= \text{Prob}\left\{\zeta_{ij}\hat{T}_{ij}l_{ijk} > \Psi\sqrt{(\hat{T}_{ij}l_{ijk})^2}\right\} \\
&\leq \exp\{-\Psi^2/2\} \\
&< \epsilon.
\end{aligned}$$

Therefore, the conditions (4.17) and (4.18) imply that the probability ϵ is not exceeded, providing an equivalent approximation of the ambiguous chance constraint (4.11).

The proof is complete. □

Equation (4.17) represents a tractable approximation of the ambiguous chance constraint (4.11) which implies that any viable solution for inequality (4.17) and (4.18) remains viable for the ambiguous chance constraint (4.11).

Thus, we express the DRO model under bounded zero-mean perturbations for the ambiguity set as follows.

[**Bounded**]

$$\min \sum_{i\in\mathcal{I}} FC_i y_i + \sum_{i\in\mathcal{I}}\sum_{k\in\mathcal{K}} VC_{ik}q_{ik} + \gamma \cdot \sum_{i\in\mathcal{I}}\sum_{j\in\mathcal{J}}\sum_{k\in\mathcal{K}} (\bar{T}_{ij} + \zeta_{ij}\hat{T}_{ij})E_{jk}x_{ijk}$$

S.t.

Constraints (4.5) to (4.10), (4.12) to (4.15), (4.17) and (4.18).

4.2.2 Solution under Gaussian perturbations

For this section, the ambiguity sets $\mathcal{P}$ consist of perturbations $\{\zeta_{ij}\}$ that are Gaussian random variables, each independent, with partially known mean expectations $\mathbf{M}[\zeta_{ij}]$ and variances $\mathbf{V}[\zeta_{ij}]$. These variables are constrained within certain bounds: $\mathbf{M}[\zeta_{ij}] \in \left[\mu_{ij}^-, \mu_{ij}^+\right]$ and $\mathbf{V}[\zeta_{ij}] \leq \sigma_{ij}^2$. Within this uncertainty range, the following observation is derived.

Theorem 4.2.2. Let $\mathbf{M}[\zeta_{ij}] \in \left[\mu_{ij}^-, \mu_{ij}^+\right]$ and $\mathbf{V}[\zeta_{ij}] \leq \sigma_{ij}^2$ where $\left[\mu_{ij}^-, \mu_{ij}^+\right]$ and σ_{ij}^2 are known. Normalizing the ambiguous chance constraint results in:

$$\bar{T}_{ij} l_{ijk} + \max\left[\mu_{ij}^- \hat{T}_{ij} l_{ijk}, \mu_{ij}^+ \hat{T}_{ij} l_{ijk}\right] + \Phi^{-1}(1-\epsilon)\sqrt{(\sigma_{ij}\hat{T}_{ij} l_{ijk})^2} \leq \theta \tag{4.20}$$

where $\Phi^{-1}(1-\epsilon)$ represents the inverse parameter of the standard normal distribution.

Proof. We will establish the equivalence of Equation (4.20) with (4.11) within the ambiguity sets $\mathcal{P}$: Let μ_{ij} and ν_{ij}^2 denote $\mathbf{M}[\zeta_{ij}]$ and $\mathbf{V}[\zeta_{ij}]$ respectively. Hence, $\mu_{ij} \in \left[\mu_{ij}^-, \mu_{ij}^+\right]$ and $\nu_{ij}^2 \leq \sigma_{ij}^2$, $\forall i, j \in \mathcal{V}, \forall k \in \mathcal{K}$. Normalizing the chance constraint

results in

$$\inf_{P\in\mathcal{P}} \text{Prob}_{\zeta\sim P}\left\{\frac{(\zeta_{ij}-\mu_{ij})}{\sqrt{(\nu_{ij}\hat{T}_{ij}l_{ijk})^2}} \leq \frac{\theta-(\bar{T}_{ij}l_{ijk}+\mu_{ij}\hat{T}_{ij}l_{ijk})}{\sqrt{(\nu_{ij}\hat{T}_{ij}l_{ijk})^2}}\right\} \geq 1-\epsilon.$$

Using the distribution function $\Phi(\cdot)$ of the standard normal distribution, we obtain

$$\Phi\left(\frac{\theta-(\bar{T}_{ij}l_{ijk}+\mu_{ij}\hat{T}_{ij}l_{ijk})}{\sqrt{(\nu_{ij}\hat{T}_{ij}l_{ijk})^2}}\right) \geq \Phi^{-1}(1-\epsilon).$$

Subsequently, for $\epsilon \leq 0.5$, we derive:

$$\frac{\theta-(\bar{T}_{ij}l_{ijk}+\mu_{ij}\hat{T}_{ij}l_{ijk})}{\sqrt{(\nu_{ij}\hat{T}_{ij}l_{ijk})^2}} \geq \Phi^{-1}(1-\epsilon).$$

Rearranging the above expression to isolate θ leads to:

$$\bar{T}_{ij}l_{ijk}+\mu_{ij}\hat{T}_{ij}l_{ijk}+\Phi^{-1}(1-\epsilon)\sqrt{(\nu_{ij}\hat{T}_{ij}l_{ijk})^2} \leq \theta.$$

Considering $\mu_{ij} \in \left[\mu_{ij}^{-}, \mu_{ij}^{+}\right]$ and $\nu_{ij}^2 \leq \sigma_{ij}^2$, we find:

$$\max\left\{\bar{T}_{ij}l_{ijk}+\mu_{ij}\hat{T}_{ij}l_{ijk}\right\}+\Phi^{-1}(1-\epsilon)\sqrt{(\nu_{ij}\hat{T}_{ij}l_{ijk})^2} \leq \theta$$

$$\implies \bar{T}_{ij}l_{ijk}+\max[\mu_{ij}^{-}\hat{T}_{ij}l_{ijk}, \mu_{ij}^{+}\hat{T}_{ij}l_{ijk}]+\Phi^{-1}(1-\epsilon)\sqrt{(\sigma_{ij}\hat{T}_{ij}l_{ijk})^2} \leq \theta.$$

This completes the proof. □

Therefore, on the basis of Theorem 4.2.2, the original ambiguous chance constraint (4.11) transforms into (4.20). Hence, the optimal solution for our DRO model can be obtained by solving the corresponding DRO model below.

[Gaussian]

$$\min \sum_{i\in\mathcal{I}} FC_i y_i + \sum_{i\in\mathcal{I}}\sum_{k\in\mathcal{K}} VC_{ik} q_{ik} + \gamma \cdot \sum_{i\in\mathcal{I}}\sum_{j\in\mathcal{J}}\sum_{k\in\mathcal{K}} (\bar{T}_{ij} + \zeta_{ij}\hat{T}_{ij}) E_{jk} x_{ijk}$$

S.t.

Constraints (4.5) to (4.10), (4.12) to (4.15), and (4.20).

Chapter 5

Results and Analysis

To showcase the efficiency of both algorithms from the previous chapter, we present two solved cases of varying sizes in this section: a hypothetical case on a small scale and a practical case on a larger scale. The optimization problems and the suggested solution strategies are coded in Python, utilizing Gurobi for solving. The computations are performed using a personal computer equipped with an Intel Core i7 2.10GHz Quad-Core processor, 8GB RAM, and operating on a 64-bit Windows 10 system.

5.1 A Hypothetical Case

Consider a hypothetical emergency response situation involving 10 possible incident sites, 4 candidate emergency facility locations, and 2 hazmat types. Because this

problem is a small-scale model, we assume that fixed costs for emergency facility placement range between \$20,000 and \$30,000, while variable costs for maintaining emergency units fall within the range of \$200 to \$600. The capacities of the facilities range between 20 and 40 units. Emergency requirements for each of the hazmat types are between 0 and 10 units for each of the incident sites. The case also includes a budget of \$105,000 which is designated for emergency facility construction. Additionally, the emergency requirements at the incident sites as well as the potential risks associated with the different hazmat types are given in Table 5.1. This case aims to optimize the deployment of emergency resources, considering various costs, capacities, varying response times, and potential risks associated with different hazmat types at distinct incident sites.

Response time from the pair of emergency facilities and incident sites is assumed to range from 1 to 20 minutes. The assumed average vehicle speed stands at 0.5 kilometers per minute. For the sake of simplicity, we assume the distances between nodes are Euclidean distances, hence the table presented in Table 5.2 portrays the average response time $\bar{T}_{ij}$ from each candidate emergency facility i to site j, while the maximum allowable response time θ is set at 7 minutes. As a result of uncertainties of response time within the system, we assume that the basic perturbation shift $\hat{T}_{ij}$ is 10% of the nominal value. In view of the situation, we assume that μ_{ij}^{-} and μ_{ij}^{+} take values in [-1, 1], and σ takes values in [0, 0.1]. To compare the different ambiguity sets, we assume that $\Psi = 2\ln(1/\epsilon) = 2.146$, where $\epsilon = 0.1$. For the inverse error

Table 5.1: Values of E_{jk} and W_{jk} for $j = 1$ to 10

Incident site j	$E_{j,1}$	$E_{j,2}$	$W_{j,1}$	$W_{j,2}$
site 1	986	280	7	0
site 2	681	505	7	2
site 3	345	943	1	8
site 4	847	389	0	8
site 5	875	628	9	8
site 6	782	156	4	5
site 7	161	747	4	9
site 8	5	568	1	8
site 9	534	659	2	0
site 10	823	595	7	2

Table 5.2: Average response time from candidate facility i to site j

$\bar{T}_{ij}$	$j = 1$	$j = 2$	$j = 3$	$j = 4$	$j = 5$	$j = 6$	$j = 7$	$j = 8$	$j = 9$	j=10
$i = 1$	9	1	6	7	4	9	8	3	2	4
$i = 2$	6	4	10	3	9	1	4	3	2	3
$i = 3$	1	6	5	4	8	5	3	1	9	4
$i = 4$	1	1	10	5	7	10	7	6	4	6

function Φ^{-1}, we calculate the inverse of the cumulative distribution function for the given probability value using a standard normal distribution $\Phi^{-1}(1 - 0.1) = 1.282$. For the sake of this computation, we assume that the risk coefficient γ is 0.1.

5.1.1 Basic Performance under Bounded zero-mean perturbations

The optimization model was solved using the Gurobi Optimizer version 10.0.3, targeting hazmat emergency logistics management considering random travel times. The optimization model comprises 574 rows, 253 columns, and 2025 nonzeros. The model has 160 quadratic constraints, 81 continuous variables, and 172 integer variables (84 binary).

The achieved optimal objective value for this case was 149,196.82 with a gap of 0.0000%. The Gurobi Optimizer took 0.05 seconds and 95 iterations to find the optimal solution. The optimal objective value was dissected into total facility cost ($100,793.0), the total cost of maintaining supplies ($30,601.0), and total risk (178,028.2). Specific values for variables were determined in the optimal solution.

The solution suggests the establishment of all four facilities (nodes 1, 2, 3, 4), the positioned emergency units for each hazmat type, and their emergency resource allocation are also determined.

5.1.2 Basic Performance under Gaussian perturbations

In this computation, the optimization process navigated through the model with 653 rows, 252 columns and 2184 nonzeros using 1 node and 70 simplex iterations, concluding in a computational time of 0.03 seconds. The model incorporated 80 quadratic constraints with variable types: 80 continuous variables and 172 integer

variables (84 binary).

The solution yields valuable insights into various decision variables. The Phi-inverse calculated during the process was 1.2816, resulting in an optimal objective value of 127,317.04. Further examination revealed the total facility cost of $76,031.0, the total cost of maintaining supplies at $29,753.0, and evaluated total risk of 215,330.4.

In this setting, the solution recommends the establishment of three facilities, while suggesting distinctive emergency unit allocations for each of the hazmat types.

5.1.3 Model Comparison

From the numerical computation, it is evident that the Gaussian perturbation problem exhibits a larger model size in terms of both rows and non-zero elements in the output, albeit with fewer quadratic constraints compared to the Bounded zero-mean perturbations problem. Notably, as seen in Table (5.3), while the optimal objective values are close, the result under the Gaussian perturbations is marginally better than the corresponding value in Bounded zero-mean perturbations. This distinction can be attributed to the fact that the model under Gaussian perturbations integrates more partial probability distribution details by including additional variance information as opposed to Bounded perturbation (Yin et al., 2019).

Additionally, Table 5.4 shows the number of units pre-positioned and maintained at each of the established facilities. We notice that four facilities (nodes 1, 2, 3,

4) and three facilities (nodes 2, 3, 4) were opened for the Bounded and Gaussian solutions respectively. In the Bounded solution, emergency facility 1 maintains 9 emergency units, facility 2 maintains 18 units, facility 3 maintains 1 unit, and facility 4 maintains 14 units for hazmat type 1. For hazmat type 2, the Bounded solution maintains 10 units at Facility 1, 0 units at Facility 2, 30 units at Facility 3, and 10 units at Facility 4. On the other hand, in the Gaussian solution, the quantities of emergency units differ slightly for hazmat types 1 and 2 at some facilities. Facility 2 maintains 21 units for hazmat type 1, compared to 18 units in the Bounded solution. Facility 3 maintains 1 unit for hazmat type 1, similar to the Bounded solution, while it maintains 38 units for hazmat type 2, differing from the 30 units in the Bounded solution. Moreover, Facility 4 maintains 20 units for hazmat type 1 and the same 10 units for hazmat type 2, differing from the Bounded solution by 6 units for hazmat type 1. Notably, for the Bounded solution, the capacities of the facilities are not fully maximized, because even though there are still unfilled capacities at the constructed facilities, positioning emergency response units in these facilities is infeasible since the incident sites are quite far away from them. As a result, more facilities are located to ensure a response time lower than the maximum allowable time is utilized. The difference observed between the quantities of emergency units maintained for the Gaussian and Bounded solutions can be attributed to the Gaussian perturbation's inherent flexibility which allows the Gaussian perturbation to explore a wider range of possibilities within the search space, potentially enabling the identification of

Table 5.3: Comparison of Objective Function Values

Perturbation	Objective Value	Facility Cost	Maintenance Cost	Risk
Bounded	149,196.82	$100,793.0	$30,601.0	178,028.2
Gaussian	127,317.04	$76,031.0	$29,753.0	215,330.4

Table 5.4: Pre-positioned units at facility i for hazmat k

Node	Facility Cost	Capacity	Hazmat type	Bounded	Gaussian
1	$24,762	21	hazmat 1	9	0
			hazmat 2	10	0
2	$20,968	28	hazmat 1	18	21
			hazmat 2	0	2
3	$28,865	39	hazmat 1	1	1
			hazmat 2	30	38
4	$26,198	30	hazmat 1	14	20
			hazmat 2	10	10

alternative, potentially more optimized response solutions.

5.1.4 Variation in tolerance levels

We conducted a sensitivity analysis by varying parameters within the models to assess their impact. Table 5.5 illustrates the influence of different tolerance levels (ϵ) on the models' uncertainty scope. Increasing ϵ values from 0.001 to 0.30 exhibited a notable sensitivity pattern, affecting both the auxiliary variable (Ψ) and the inverse error function for the confidence level ($\Phi^{-1}(1-\epsilon)$). Specifically, as the tolerance

Table 5.5: Parameter values for different tolerance levels

ϵ	0.001	0.01	0.05	0.1	0.15	0.2	0.25	0.3
Ψ	3.7169	3.0349	2.4477	2.1460	1.9479	1.7941	1.6651	1.5518
$\Phi^{-1}(1-\epsilon)$	3.0902	2.3263	1.6449	1.2816	1.0364	0.8416	0.6745	0.5244

level increased, a consistent decreasing trend emerged for Ψ, declining from 3.72 to 1.55. Similarly, $\Phi^{-1}(1-\epsilon)$ experienced a reduction from 3.09 to 0.52. These changes signify that higher tolerance levels correspond to decreased Ψ and $\Phi^{-1}(1-\epsilon)$ values, indicating a broader ambiguity set and widening the set of potential values within the confidence interval.

To further demonstrate the effect of tolerance level on the model solutions, we solve the proposed models with varying values of ϵ. Regarding the Bounded Solution, a negligible difference of 32.23 was observed between $\epsilon = 0.20$ and 0.25 due to the risk value change as shown in Table 5.6. On the other hand, the Gaussian Solution maintained unchanging values across the different ϵ levels, showcasing stability and reliability under varying tolerance levels. Thus, while the auxiliary variable and the inverse error function of the standard normal distribution change with varying tolerance levels, the actual objective values portray a consistent and reliable optimal solution regardless of the confidence level considered.

Table 5.6: Tolerance levels and corresponding objective values

Tolerance level						
ϵ	0.001	0.01	0.10	0.20	0.25	0.30
Bounded Solution						
O	149,196.82	149,196.82	149,196.82	149,196.82	149,164.59	149,164.59
F	100,793.00	100,793.00	100,793.00	100,793.00	100,793.00	100,793.00
V	30,601.00	30,601.00	30,601.00	30,601.00	30,567.00	30,567.00
R	178,028.20	178,028.20	178,028.20	178,028.20	178,045.90	178,045.90
Gaussian Solution						
O	127,317.04	127,317.04	127,317.04	127,317.04	127,317.04	127,317.04
F	76,031.00	76,031.00	76,031.00	76,031.00	76,031.00	76,031.00
V	29,753.00	29,753.00	29,753.00	29,753.00	29,753.00	29,753.00
R	215,330.40	215,330.40	215,330.40	215,330.40	215,330.40	215,330.40

Where O: Objective Value, F: Facility Cost, V: Maintenance Cost, R: Risk

5.1.5 Variation in the Risk Coefficient

Considering the importance of risk reduction in the optimization problem and changing the risk coefficient γ from 0.1 to 2, we analyze the proposed models for $\epsilon = 0.1$ and a specified θ of 7 minutes. The comparison between the Bounded and Gaussian solutions produces the following optimization outcomes. As seen in Table 5.7, the Bounded solution, despite providing better total risk values compared to the Gaussian solution, still produces substantially higher emergency facility and maintenance costs (combined as cost) in comparison. This trend potentially indicates a

Table 5.7: Results for different γ values

γ	Bounded		Gaussian	
	Cost	Risk	Cost	Risk
0.1	131,394	178,028.20	105,784	215,330.36
0.5	133,808	169,810.76	107,493	204,909.14
1	136,571	165,841.34	136,394	165,867.54
2	137,810	164,668	137,633	164,694.20

more conservative approach taken by the Bounded solution, prioritizing risk mitigation strategies at the expense of the overall objective value. On the other hand, the Gaussian solution, while yielding slightly higher risk values, showcases a more cost-efficient approach, resulting in reduced costs. Hence, this incurred higher risk suggests a comparatively greater tolerance for risk in the Gaussian solution, emphasizing potential trade-offs between cost reduction and risk management within the optimization process. Interestingly, the Gaussian model still produced better solutions overall for the analyzed results. The increase in cost with increasing γ suggests that placing more importance on risk results in higher costs, possibly due to the implementation of risk mitigation measures.

Furthermore, Fig. 5.1 illustrates the behavior of both models with the cost and risk values compared for Bounded and Gaussian models. This analysis highlights the inverse relationship between the risk objective and cost objective, with the Bounded model consistently exhibiting higher costs and lower risks compared to the Gaussian model.

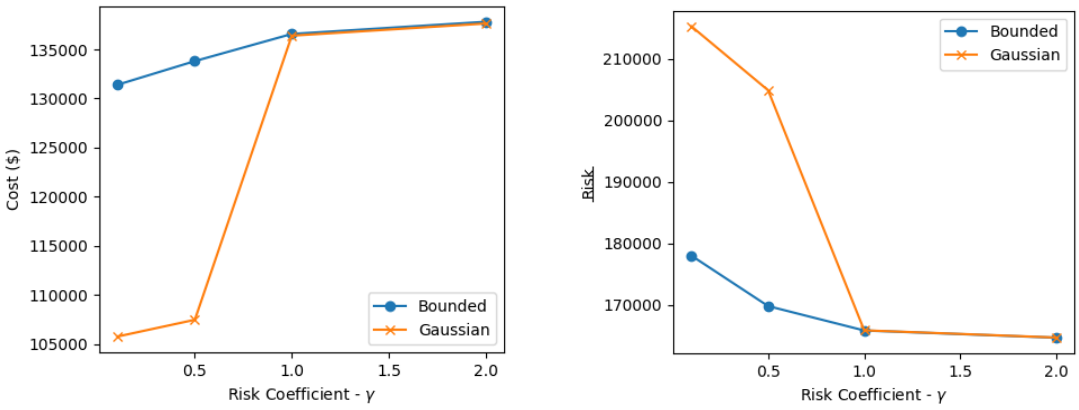

(a) Cost performance

(b) Risk performance

Figure 5.1: Cost and Risk percentages for different γ values

5.1.6 Variation in the Maximum Response Time

For the models, we fix the tolerance level ϵ at 0.1, vary the value of θ from 6 to 10 minutes, and analyze the resulting solutions. Starting with the Bounded solution, various values of θ lead to notable changes in the optimization results. At 6 minutes, the solution is infeasible, indicating that there are no timely links below θ to sustain the system. Increasing the value from 7 minutes to 8 minutes results in a minor reduction in the optimal objective value while maintaining the number of facilities constructed. However, a more significant impact is observed when transitioning to maximum allowable time values of 9 minutes and 10 minutes, which leads to a reduction in the optimal objective value and a subsequent decrease in both total facility cost and total maintenance costs. Interestingly, this decrease is accompanied by an increase in the total risk, suggesting that higher θ values might lead to the

establishment of fewer facilities.

On the other hand, the Gaussian solution presents slight changes for the tested values of θ, while maintaining better optimal solutions compared to its Gaussian counterpart. Increasing the value from 6 to 7 minutes returned significant results, reducing the objective value by over \$21,000 as well as the number of constructed facilities from 4 to 3. Varying the maximum time between 7 to 9 minutes resulted in no reduction in the optimal objective value and configurations. However, a slight impact was observed at a maximum allowable time of 10 minutes, which led to a reduction in the optimal objective value with slight changes in both total facility cost and total maintenance costs. Interestingly, these observations highlight the delicate balance between the joint objectives in the problem setting. Thus the choice of θ influences not only the achieved objective value but also the number of facilities to construct and the trade-off between cost efficiency and risk mitigation. Table 5.8 presents the details.

Table 5.8: Comparison of Bounded and Gaussian Solutions for different θ Values

Perturbation	θ	Obj Value	Facility Cost	Maintenance	Risk	Facilities
Bounded	6	-	-	-	-	-
	7	149,196.82	$100,793.0	$30,601.0	178,028.20	4
	8	149,164.59	$100,793.0	$30,567.0	178,045.90	4
	9	127,317.04	$76,031.0	$29,753.0	215,330.40	3
	10	127,317.04	$76,031.0	$29,753.0	215,330.40	3
Gaussian	6	149,164.60	$100,793.0	$30,567.0	178,046.00	4
	7	127,317.04	$76,031.0	$29,753.0	215,330.40	3
	8	127,317.04	$76,031.0	$29,753.0	215,330.40	3
	9	127,317.04	$76,031.0	$29,753.0	215,330.40	3
	10	127,137.37	$76,031.0	$29,354.0	217,523.70	3

5.2 A Real-world Case Study

To demonstrate the applicability of the previously discussed models in the context of hazmat emergency response, we employ a real-world city network.

5.2.1 Network Data

Specifically, we employ the urban area of Daojiao in southeastern China for our case study. The network's data, originally sourced from Zhao and Ke (2019), Ke (2022) and Ke and Bookbinder (2023) with necessary adjustments, covers approximately 54 square kilometers. Daojiao annually produces approximately 7,950 tons of hazardous waste, necessitating an effective emergency response strategy. This analysis encom-

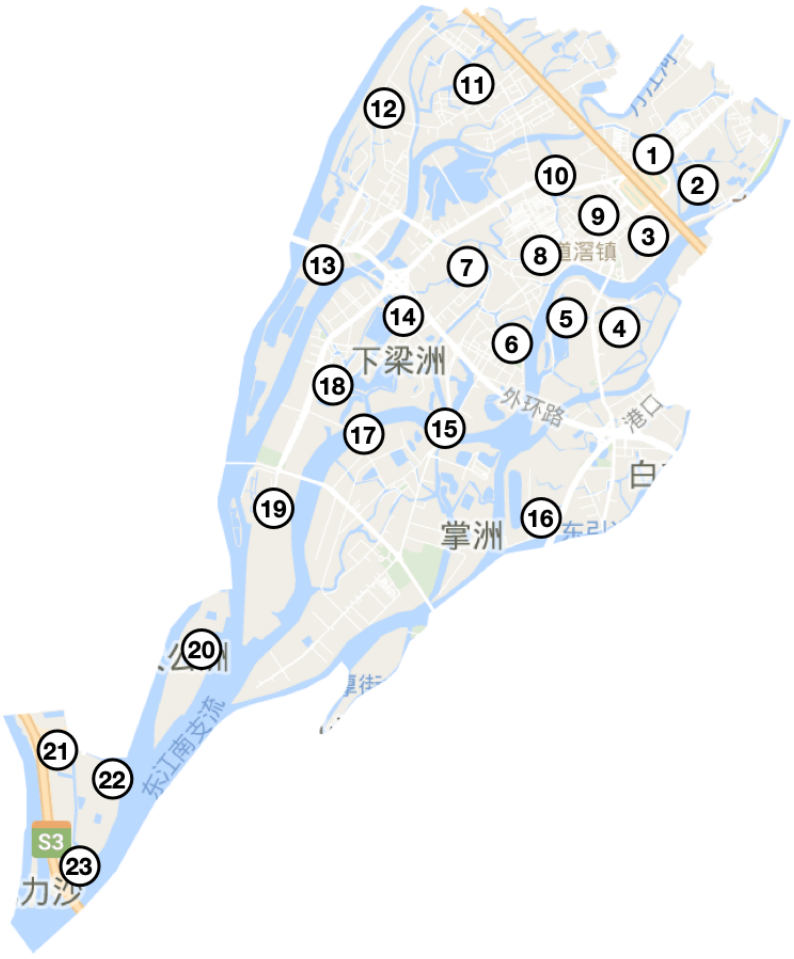

Figure 5.2: Visualization of the Daojiao city network [Adapted from Ke (2022)]

passes 106 potential incident sites, including industrial factories, hospitals, schools, residential areas, etc., which are categorized into 23 nodes based on travel time (5.2).

5.2.1.1 Risk

Within the above framework, the study considers three distinct hazmat types: used oil, explosive waste, and waste organic solvent. Each hazmat type has an impact

radius of 0.5 km, 0.8 km, and 1.6 km, respectively, defining the surrounding danger zones. The average hazmat amounts generated at these sites total around 75 tons per type, with a 50% variation, as indicated by Zhao and Ke (2019). These quantities are then integrated into the 23 nodes, forming the basis for our comprehensive analysis. The hazmat risk estimation for each node is calculated based on a worst-case scenario, taking into account cumulative time-based population exposure within each zone. This estimation considers zone size, population density, and hazmat quantity, while the base risk coefficient γ is set at 0.01.

5.2.1.2 Cost

The determination of candidate emergency facility locations and their capacities involves a meticulous analysis of required emergency resources and network connections. As a result, twelve potential locations are identified, comprising six small, four medium, and two large facilities. Table 5.9 presents key cost and capacity details for these candidate facilities. Construction cost estimates are derived from the Construction and Development Guide recommended by the Chinese National Registered Architect Management Committee (1995) and Ministry of Transport of the People's Republic of China (2018), adjusted for inflation in RMB[1]. Cost for maintaining a single emergency unit at any emergency facility amounts to 25,000 RMB, while available budget for emergency facility construction is set to an initial value of 90 million

[1]RMB stands for Renminbi, the currency of the People's Republic of China, worth about 0.19 of a Canadian dollar in August, 2024.

Table 5.9: Candidate facility information in the Daojiao city network (Ke, 2022)

Facility	Candidates #	Capacity	Fixed Cost ($\times 10^4$ RMB)
Small	6, 9, 15, 18, 20, 22	50	600
Medium	2, 8, 11, 12	70	800
Large	4, 14	100	1,000

RMB, which is sufficient for constructing the maximum number of facilities should there be need. We set this value to allow the model enough flexibility to solve the hazmat emergency problem even in scenarios of extreme uncertainty.

5.2.1.3 Response time

The average response time within a pair of nodes is determined by the time taken to traverse Euclidean distances at a standardized speed of 0.5 km per minute. To account for uncertainties in response time, a basic perturbation shift ($\hat{T}_{ij}$) of 20% from the nominal value is assumed. The model incorporates these uncertainties by considering mean expectation ranges (μ_{ij}^- and μ_{ij}^+) between -1 and 1, while σ takes values in the interval [0, 0.5].

Computational simulations for this case study are executed on an Intel Core i7 2.10GHz Quad-Core processor with 8GB RAM, running a 64-bit Windows 10 operating system.

Table 5.10: Bounded model with different cases of ϵ and θ

Case	ϵ	θ	No. of facilities	Cost ($\times 10^4$ RMB)		Risk ($\times 10^5$)	CPU time (s)
				Fixed Cost	Maint Cost		
B11	0.001	8	-	-	-	-	-
B12		9	9	6,200	927.5	4,199	0.31
B13		10	9	6,200	927.5	4,199	0.93
B14		12	8	5,600	927.5	5,538	1.42
B15		15	6	4,400	927.5	5,756	1.93
B16		20	5	4,200	927.5	4,813	2.45
B21	0.1	8	9	6,200	927.5	4,199	0.39
B22		9	8	5,600	927.5	5,538	0.94
B23		10	8	5,600	927.5	5,538	1.61
B24		12	6	4,400	927.5	5,756	2.09
B25		15	5	4,200	927.5	4,813	2.52
B26		20	5	4,200	927.5	4,806	3.36
B31	0.3	8	8	5,600	927.5	5,538	1.19
B32		9	8	5,600	927.5	5,538	1.26
B33		10	7	5,000	927.5	4,699	1.53
B34		12	5	4,200	927.5	5,791	1.55
B35		15	5	4,200	927.5	4,813	1.95
B36		20	5	4,200	927.5	4,580	2.31

5.2.2 Bounded model

We solve the Bounded model in several cases with different tolerance levels ($\epsilon = 0.0001, 0.1, 0.3$) and distinct maximum allowable response times. The outcomes, including the costs, risk, and computational durations are presented in Table 5.10.

Examining the outcomes, it is evident that as the tolerance level increases, the costs and risk values exhibit a unique pattern across cases with similar maximum allowable response times. For instance, comparing cases B13, B23, and B33 for the maximum allowable time of 10 minutes, we observe variations in the number of facilities, costs, and risks. At a tight tolerance in case B13, the network produced the worst fixed cost value of 6,200 $\times 10^4$ RMB and a relatively high number of facilities (9). As the tolerance value is increased from 0.001 towards 0.3, we observe that cases B23 and B33 present better fixed cost results of 5,600 $\times 10^4$ RMB and 5,000 $\times 10^4$ RMB respectively for both cases, improving significantly. The number of facilities also decrease to 8 and 7 respectively in both cases, indicating potential cost optimization. The results underscore the need to construct more facilities as the tolerance level is reduced. As a result of the low tolerance level, more facilities are constructed to meet the confidence requirement. The computational duration shows an increasing trend as the values of θ increase and indicate reasonably efficient computational performance in handling our network size. In evaluating the variations in the network performance based on the maximum allowable response time, we observe the model's behavior with different θ values for different tolerance situations. Taking $\epsilon = 0.001$ for instance, in analyzing cases B11 to B16, B11 returns no feasible solution in th egiven tolerance level for the problem. Further, B12 presents the worst performance at θ of 9 minutes, with 6,200 $\times 10^4$ RMB fixed facility cost and 9 facilities. As the maximum allowable response time increases from 9 to 20, we observe

the subsequent cases (B13 to B16) exhibit better improvements in their cost values. Notably, the total cost of maintaining emergency units (Maint. cost) across all cases stayed the same, signifying consistency in the total number of emergency groups maintained for each solution, irrespective of the emergency facility and allocation configurations. The unique interaction between cost and risk is also obvious, showing risk increases in certain cases as a result of suppressed emergency facility construction costs.

Furthermore, we evaluate the solutions in this model to understand the positioning of emergency units within the model. We highlight three cases B12, B22 and B32 from the solved cases, and present their outcome in below Table 5.11[2]. To prove the accuracy of the solutions, the total number of emergency units pre-positioned across the cases tallied with the total emergency demand across the system (371 units), with no redundancy.

5.2.3 Gaussian model

Similarly, the Gaussian model is applied to optimize the network under the three cases of ϵ. Table 5.12 provides comprehensive insights into the model's performance across different optimization cases.

Solving the model for a given tolerance level across different maximum allowable times results in varying fixed cost and risk values, as well as different number of

[2]we use "x" in our tables to show that an emergency facility is opened.

Table 5.11: Bounded emergency response groups per facility ($\theta = 9$)

Case	Facility candidates	Facility capacity	Opened facility	Hazmat type			Total
				1	2	3	
B12	1	50	x	15	12	13	40
	2	70	x	19	13	24	56
	4	100	x	31	11	17	59
	8	70	x	31	21	10	62
	9	50	x	25	3	22	50
	11	70	-	-	-	-	-
	12	70	-	-	-	-	-
	14	100	-	-	-	-	-
	15	50	x	10	12	9	31
	18	50	x	3	0	7	10
	20	50	x	1	0	12	13
	22	50	x	21	19	10	50
							371
B22	1	50	x	15	19	16	50
	2	70	-	-	-	-	-
	4	100	x	39	11	29	79
	8	70	x	31	21	10	62
	9	50	x	23	0	27	50
	11	70	-	-	-	-	-
	12	70	x	21	10	18	49
	14	100	-	-	-	-	-
	15	50	x	7	15	9	31
	18	50	x	3	0	12	15
	20	50	-	-	-	-	-
	22	50	x	17	15	3	35
							371
B32	1	50	x	15	19	16	50
	2	70	-	-	-	-	-
	4	100	x	39	11	29	79
	8	70	x	31	21	10	62
	9	50	x	23	0	27	50
	11	70	-	-	-	-	-
	12	70	x	21	10	18	49
	14	100	-	-	-	-	-
	15	50	x	7	15	9	31
	18	50	x	3	0	12	15
	20	50	-	-	-	-	-
	22	50	x	17	15	3	35
							371

Table 5.12: Gaussian model with different cases of ϵ and θ

Case	ϵ	θ	No. of facilities	Cost ($\times 10^4$ RMB)		Risk ($\times 10^5$)	CPU time (s)
				Fixed Cost	Maint Cost		
G11	0.001	8	7	5,400	927.5	6,339	0.94
G12		9	7	5,000	927.5	4,768	1.45
G13		10	6	4,400	927.5	5,745	1.42
G14		12	5	4,200	927.5	4,813	1.12
G15		15	5	4,200	927.5	4,813	1.68
G16		20	5	4,200	927.5	4,802	2.36
G21	0.1	8	7	5,000	927.5	6,923	0.96
G22		9	6	4,400	927.5	5,756	1.23
G23		10	6	4,400	927.5	5,531	1.59
G24		12	5	4,200	927.5	4,813	1.50
G25		15	5	4,200	927.5	4,813	2.02
G26		20	5	4,200	927.5	4,439	2.81
G31	0.3	8	7	5,000	927.5	4,699	1.12
G32		9	6	4,400	927.5	5,542	1.44
G33		10	6	4,400	927.5	5,531	1.58
G34		12	5	4,200	927.5	4,813	1.37
G35		15	5	4,200	927.5	4,813	2.92
G36		20	5	4,200	927.5	4,439	3.40

constructed facilities, improving in most cases as θ is increased. For instance, at $\epsilon = 0.001$, the results from cases G11 to G16 demonstrate the inherent trade-offs between flexibility in response time, cost, and risk management, improving the fixed costs across the θ values from 5,400 $\times 10^4$ RMB to 4,200 $\times 10^4$ RMB. Note that between the specified tolerance values of 0.1 and 0.3, the solutions of θ 15 to 20 minutes

become consistent to denote that the tolerance value at these points may not significantly impact the network's performance across each θ value. The computational durations from our results range from 0.94 to 3.40 seconds, indicating a moderate computational burden. On the other hand, in comparing the cases across different ϵ values, it is evident that relaxing tolerance levels generally leads to better outcomes. For instance, increasing ϵ along cases G12, G22 and, G32 yields improving objective values and suggests the establishment of 7, 6 and, 6 facilities respectively. Similar to the bounded model, the total cost of maintaining emergency units across all cases remains constant.

To further understand the outcome of this solution with respect to the maintained emergency units at each constructed emergency facility, we look at corresponding solutions from cases G12, G22 and G32 and present their results in Table 5.13[3]. Obviously, the model suggests different configurations for the analysed cases, while retaining accurate total emergency pre-positioned units (371 units) across the analyzed cases.

5.2.4 Variation in the Risk Coefficient

Our model's combined objectives are cost and risk, which are linked by a risk coefficient γ enabling an interaction between both. To have a better view of this analysis, we simplify our presentation of cost in this section by adding both the emergency

[3]we use "x" in our tables to show that an emergency facility is opened.

Table 5.13: Gaussian emergency response groups per facility ($\theta = 9$)

Case	Facility candidates	Facility capacity	Opened facility	Hazmat type			Total
				1	2	3	
G12	1	50	x	13	17	20	50
	2	70	-	-	-	-	-
	4	100	x	39	11	29	79
	8	70	-	-	-	-	-
	9	50	x	25	15	10	50
	11	70	-	-	-	-	-
	12	70	-	-	-	-	-
	14	100	x	38	22	32	92
	15	50	-	-	-	-	-
	18	50	x	3	5	11	19
	20	50	x	15	4	12	31
	22	50	x	23	17	10	50
							371
G22	1	50	x	14	9	27	50
	2	70	-	-	-	-	-
	4	100	x	41	13	29	83
	8	70	-	-	-	-	-
	9	50	x	24	15	11	50
	11	70	-	-	-	-	-
	12	70	-	-	-	-	-
	14	100	x	38	22	31	91
	15	50	-	-	-	-	-
	18	50	x	16	15	16	47
	20	50	-	-	-	-	-
	22	50	x	23	17	10	50
							371
G32	1	50	x	4	19	27	50
	2	70	-	-	-	-	-
	4	100	x	51	13	29	93
	8	70	-	-	-	-	-
	9	50	x	24	15	11	50
	11	70	-	-	-	-	-
	12	70	-	-	-	-	-
	14	100	x	38	22	31	91
	15	50	-	-	-	-	-
	18	50	x	16	5	16	37
	20	50	-	-	-	-	-
	22	50	x	23	17	10	50
							371

Table 5.14: Variation in Risk Coefficient

γ	Bounded			Gaussian		
	Cost ($\times 10^4$ RMB)	Risk ($\times 10^5$)	# of facilities	Cost ($\times 10^4$ RMB)	Risk ($\times 10^5$)	# of facilities
0.01	6,527.5	5,538	8	5,327.5	5,756	6
0.1	7,727.5	1,908	9	5,727.5	3,440	6
0.25	7,727.5	1,908	9	7,127.5	2,075	8
0.5	8,327.5	1,722	10	8,327.5	1,722	10
0.75	9,727.5	1,573	11	9,727.5	1,573	11
1	9,727.5	1,500	12	9,727.5	1,500	12

facility cost and the emergency maintenance costs together. We then look at corresponding solutions where θ is 9 minutes for different γ values with respect to both Bounded and Gaussian models from cases B22 and G22 respectively. We present the values associated with the cost and risk objectives in Table 5.14.

Notably, as γ rises, corresponding results from both models change at different rates denoting their response to the varying risk weight. As the risk coefficient increases, we see that a decision maker that values risk more highly, will spend more to reduce risk. As a result, a higher number of selected facilities is recorded as well to corroborate the optimization effort. For instance, at a low γ of 0.01 from the Bounded model, the cost is 6,527.5 $\times 10^4$ RMB, whereas, at $\gamma = 0.1$, the cost rises to 7,727.5 $\times 10^4$ RMB. On the other hand, the Gaussian model produces a better total cost value of 5,327.5 $\times 10^4$ RMB at $\gamma = 0.01$ which is consistent with our earlier

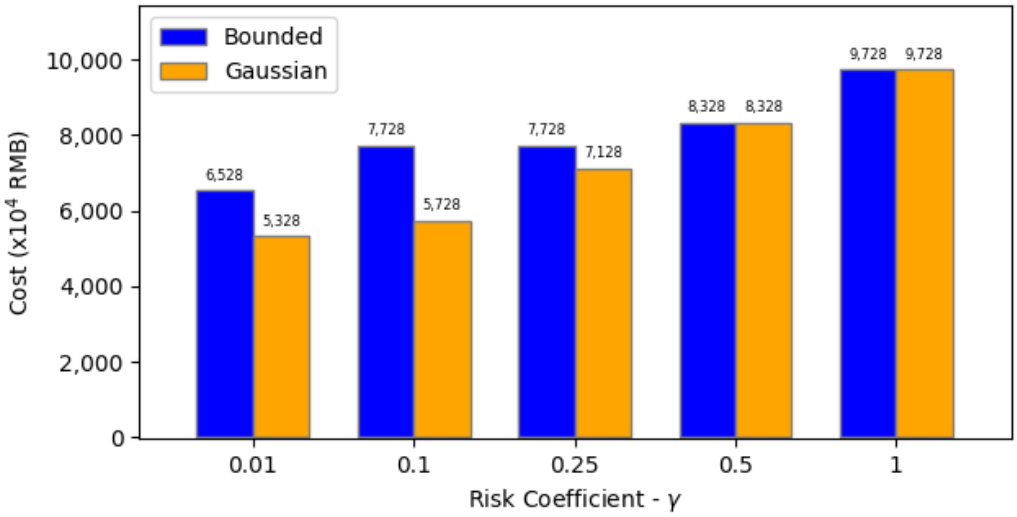

Figure 5.3: Cost values with different γ values

results. However, we observe that as γ values rise, the difference between the two models gets smaller and smaller until convergence is recorded with both models at $\gamma = 0.5$. At $\gamma = 1$, all the candidate facilities within the network are selected and any increase in γ above 1 will retain equilibrium in both models. Consistent with our previous case, the Bounded model consistently exhibits higher costs and lower risks compared to the Gaussian model, except at $\gamma = 0.5$ and above where both values are the same. The details of the cost and risk outcomes are presented in Fig. 5.3 and Fig. 5.4, respectively. Fig. 5.5 shows the number of facilities constructed as various values of γ shifts the problem focus from the cost objective to the risk objective.

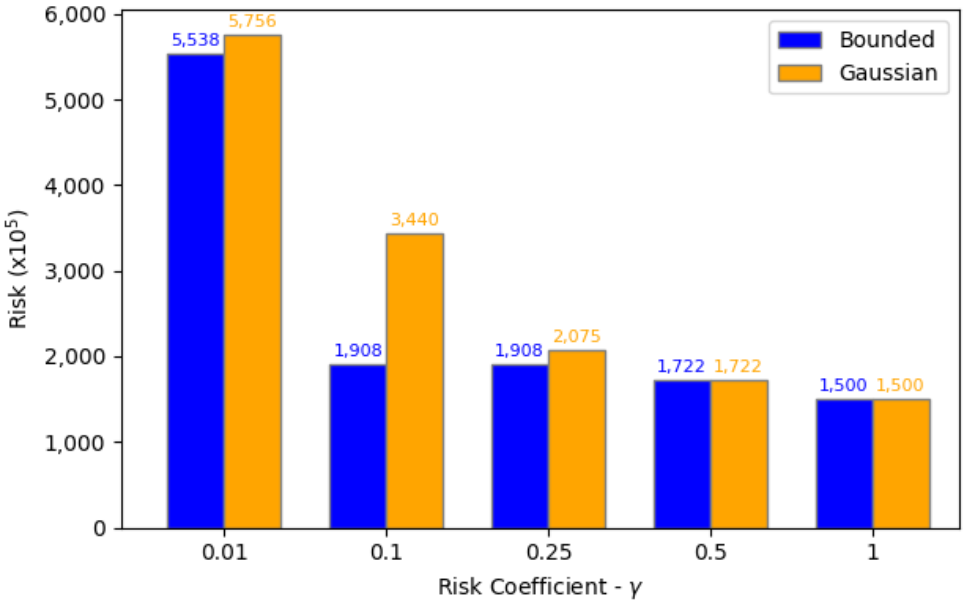

Figure 5.4: Risk values with different γ values

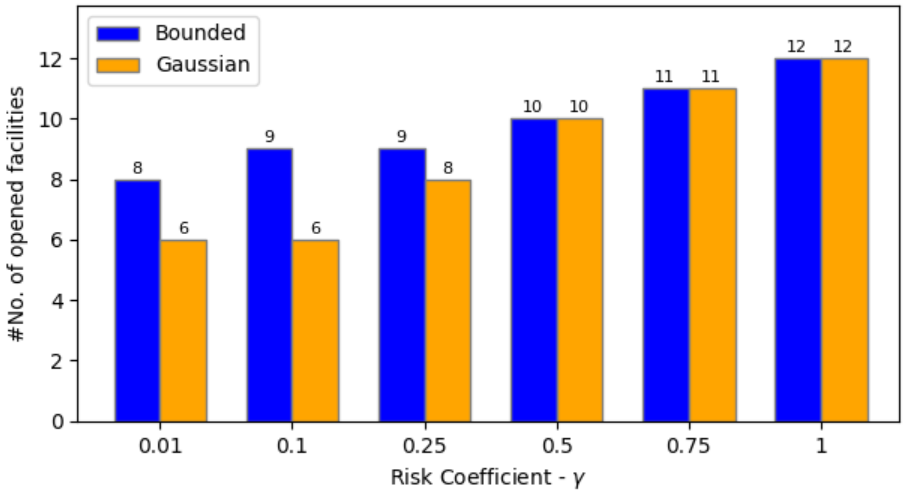

Figure 5.5: Opened facilities with respect to γ

5.2.5 Variation in Gaussian Variances

In this section, we perform sensitivity analysis on the Gaussian model to understand how changes in σ impact the optimization results. Varying the range of σ will vary the level of variability within the system. We select case G12 for this analysis and present the results in Table 5.15. From the table, as we increase σ, we see that the optimization model tends to produce more conservative solutions to account for the increased variability in the uncertain parameter. For instance, as we set σ to take random values within the range [0, 2], we see the total cost value rise to 7,127.5 $\times 10^4$ RMB. This pattern aligns with the expectation that higher uncertainty prompts the model to generate more conservative solutions, emphasizing robustness at the expense of increased costs. Concurrently, the number of constructed emergency facilities displays a noticeable increase with higher values of σ, indicating the model's response to elevated uncertainty. This behavior adheres to the principles of our optimization model, where additional facilities are strategically positioned to enhance the system's resilience against a broader spectrum of potential perturbations. The observed trade-off between robustness and cost management is apparent in the results. Lower values of σ correspond to lower costs but potentially expose the system to higher risk. In contrast, higher values of σ lead to more conservative solutions, with increased costs and a higher number of facilities, bolstering the system's robustness against uncertainties.

Table 5.15: Variation in Gaussian Variances (Case G13)

σ interval	Cost ($\times 10^4$ RMB)	Risk ($\times 10^5$)	# No of facilities
0 - 0.01	5,327.5	5,542	6
0 - 0.1	5,327.5	5,542	6
0 - 0.5	5,927.5	4,768	7
0 - 1	6,527.5	4,961	8
0 - 2	7,127.5	4,199	9

5.2.6 Comparison with Different Optimization Models

In this section, we compare the DRO method with the Deterministic (DET) and Robust Optimization (RO) models to provide insights into their respective solutions. We first present the deterministic model's results, followed by an analysis of the robust optimization method. Finally, we discuss how uncertainties impact the system's performance under various scenarios.

5.2.6.1 Deterministic Model Development

The deterministic optimization model aims to optimize facility locations and resource allocations under known conditions without considering uncertainties. We solve the deterministic counterpart (Section 3.4) of the model computations presented in the previous sections. The solution as shown in Table 5.18 showcases the model's ability to identify an exact optimal solution under ideal conditions. The establishment of 5 strategically positioned facilities is sufficient to cover all the network's emergency

Table 5.16: Deterministic emergency response groups per facility ($\theta = 9$)

Facility candidates	Facility capacity	Opened facility	Hazmat type			Total
			1	2	3	
1	50	-	-	-	-	-
2	70	x	27	15	28	70
4	100	x	46	13	25	84
8	70	-	-	-	-	-
9	50	-	-	-	-	-
11	70	-	-	-	-	-
12	70	x	29	23	18	70
14	100	x	38	22	37	97
15	50	-	-	-	-	-
18	50	-	-	-	-	-
20	50	x	16	18	16	50
22	50	-	-	-	-	-
						371

response requirements, as long as no disruption exists and all factors are known. We also explore the positioning of emergency units and present the result in Table 5.16.

5.2.6.2 Robust Optimization Model Development

As outlined in the literature review, the Robust Optimization (RO) method is tailored to handle uncertain parameters with known support, eliminating the need for precise probability distribution information. That is, it accommodates a set of conceivable uncertain scenarios within defined bounds, aiming to optimize solutions robust enough to perform well under the worst-case scenarios (Ben-Tal and Nemirovski, 2000). Thus, when the tolerance level (ϵ) is set to zero, a specific form of our ambiguous chance constraint emerges which ensures that the left-hand terms involving the

uncertain parameter ζ, under a given probability distribution P, remain less than or equal to the allowable time threshold θ

$$\text{Prob}_{\zeta \sim P}\left\{\bar{T}_{ij} l_{ijk} + \zeta_{ij} \hat{T}_{ij} l_{ijk} \leq \theta\right\} = 1. \tag{5.1}$$

Consistent with traditional RO theory, the worst-case scenario involves considering the perturbation variable at its maximum value within the defined support interval (Yin et al., 2019). Consequently, an equivalent robust counterpart model can be derived, and the optimal solution for the RO model can be obtained by solving the inequality

$$\max_{\zeta \sim P}\left\{\bar{T}_{ij} l_{ijk} + \zeta_{ij} \hat{T}_{ij} l_{ijk}\right\} \leq \theta. \tag{5.2}$$

The RO method produces an optimal solution categorized into facility cost: 6,200 $\times 10^4$ RMB, cost of maintaining supplies: 927.5 $\times 10^4$ RMB, and total risk: 6,602 $\times 10^5$. As shown in Table 5.18, the model recommends the construction of 9 emergency facilities which ensures the system is robust enough to perform well under the worst-case scenario. We further explore the RO method to understand the positioning of emergency units within the model and present their outcome in Table 5.17.

5.2.6.3 Comparison with Robust Optimization model

In this section, we compare the DRO method with the RO method, comparing the values obtained from both models to provide insights from their respective solutions,

Table 5.17: Robust emergency response groups per facility ($\theta = 9$)

Facility candidates	Facility capacity	Opened facility	Hazmat type			Total
			1	2	3	
1	50	x	15	12	13	40
2	70	x	19	13	24	56
4	100	x	31	11	17	59
8	70	x	31	21	10	62
9	50	x	25	3	22	50
11	70	-	-	-	-	-
12	70	-	-	-	-	-
14	100	-	-	-	-	-
15	50	x	10	12	9	31
18	50	x	3	0	7	10
20	50	x	1	0	12	13
22	50	x	21	19	10	50
						371

primarily in cost and risk behaviors as seen from Table 5.18. The Bounded model presents a high cost value of 7,127.5 $\times 10^4$ RMB for very tight tolerance while maintaining consistent values of 6,527.5 $\times 10^4$ RMB for $\epsilon = 0.1$ and 0.3. In the Gaussian model, the cost value returns 5,927.5 $\times 10^4$ RMB for $\epsilon = 0.001$, and 5,327.5 $\times 10^4$ RMB for both $\epsilon = 0.1$ and 0.3. As expected, the Robust model maintains a constant cost value at 7,127.5 $\times 10^4$ RMB, reinforcing a risk-averse approach in hazmat emergency response planning. The analysis reveals that the optimal cost of the Bounded model equals the robust optimization model only when the tolerance level ϵ is equal to 0.001. In all other instances, DRO models yield lower system costs compared to the RO model.

Turning our attention to risk considerations, the Bounded model displays an

Table 5.18: System Development Under Different models ($\gamma = 0.01$)

ϵ	Model	Cost ($\times 10^4$ RMB)	Risk ($\times 10^5$)	# of facilities	Opened facilities
-	DET	5,127.5	5,395	5	2, 4, 12, 14, 20
-	Robust	7,127.5	6,602	9	1, 2, 4, 8, 9, 15, 18, 20, 22
0.001	Bounded	7,127.5	4,199	9	1, 2, 4, 8, 9, 15, 18, 20, 22
	Gaussian	5,927.5	4,768	7	1, 4, 9, 14, 18, 20, 22
0.1	Bounded	6,527.5	5,538	8	1, 4, 8, 9, 15, 18, 20, 22
	Gaussian	5,327.5	5,756	6	1, 4, 9, 14, 18, 22
0.3	Bounded	6,527.5	5,538	8	1, 4, 8, 9, 15, 18, 20, 22
	Gaussian	5,327.5	5,542	6	1, 4, 9, 14, 18, 22

intriguing trend. The risk values increase from 4,199 $\times 10^5$ to 5,538 $\times 10^5$ as the constructed facilities are decreased from 9 to 8. This indicates a trade-off between constructing facilities and risk reduction as tolerance increases. In the Gaussian model, risk values exhibit variability, increasing from 4,768 $\times 10^5$ at $\epsilon = 0.001$ to 5,756 $\times 10^5$ at $\epsilon = 0.1$, followed by a decrease to 5,542 $\times 10^5$ at $\epsilon = 0.3$. This fluctuation in risk values suggests a delicate balance in facility construction, attempting to offset one facility from the suggested 7 at lower ϵ levels. Meanwhile, the Robust model maintains higher risk values than both DRO models at 6,602 $\times 10^5$, reinforcing a risk-averse approach in hazmat emergency response planning.

Subsequently, we compare the optimal values obtained from the DRO models and those from the RO model, presenting the objective function values and number of constructed facilities for the different models under different levels of γ. When

γ is set to 0.01 as shown in Table 5.19, the objective function values vary significantly across different models. The DET model yields an objective function value of 5,667 $\times 10^4$. This model does not account for uncertainties, resulting in a lower objective value compared to other models that incorporate risk factors. The RO model has a higher objective function value of 7,788 $\times 10^4$. This indicates that the robust approach, which considers worst-case scenarios, leads to higher costs due to the conservative nature of the model. The analysis reveals that in all ϵ instances, DRO models yield lower values compared to the RO model. This finding aligns with established conclusions, indicating that the DRO model steers clear of overly conservative solutions due to the additional probabilistic information regarding uncertain parameters. Furthermore, it achieves a lower cost, demonstrating its practical desirability in problem-solving. To facilitate clear comparisons, we depict the optimal values of the Bounded, Gaussian, and RO models in Figure 5.6.

Observing Table 5.20 for $\gamma = 0.1$, again the objective function values show clear distinctions in performance. The DET model yields an objective function value of 8,788 $\times 10^4$, while the RO model has a higher value of 10,683 $\times 10^4$, reflecting its conservative approach. Among the DRO models, the Bounded model shows higher objective function values than the Gaussian model, despite lower risk (Figure 5.7). The Gaussian model achieves lower construction costs and better optimal values overall, demonstrating its efficiency in managing distributional ambiguity. Across all the models, we observe lower risk values compared to the $\gamma = 0.01$, as a result of

Table 5.19: Computational results of various models ($\gamma = 0.01$)

ϵ	Model	Cost ($\times 10^4$ RMB)	Risk ($\times 10^5$)	Objective function ($\times 10^4$)	# of facilities
-	DET	5,127.5	5,395	5,667	5
-	Robust	7,127.5	6,602	7,788	9
0.001	Bounded	7,127.5	4,199	7,547	9
	Gaussian	5,927.5	4,768	6,404	7
0.1	Bounded	6,527.5	5,538	7,081	8
	Gaussian	5,327.5	5,756	5,903	6
0.3	Bounded	6,527.5	5,538	7,081	8
	Gaussian	5,327.5	5,542	5,882	6
0.4	Bounded	5,927.5	4,768	6,404	7
	Gaussian	5,327.5	5,542	5,882	6
0.5	Bounded	5,927.5	4,768	6,404	7
	Gaussian	5,327.5	5,542	5,882	6

increased focus towards the risk objective.

At $\gamma = 1$, the objective function values exhibit a slightly different result. The DET model's objective function value increases to 24,195 $\times 10^4$ with all 12 facilities constructed. This substantial rise reflects the heightened sensitivity to risk management when γ is higher, which is consistent with our previous studies (Section 5.2.4). Similarly, the robust model's objective function value increases to 32,875 $\times 10^4$ with 12 constructed facilities. Across all values of ϵ, both the Bounded and Gaussian models have an identical objective function value of 24,723 $\times 10^4$ with all facilities constructed (Figure 5.8. In line with Section 5.2.4, this uniformity suggests that

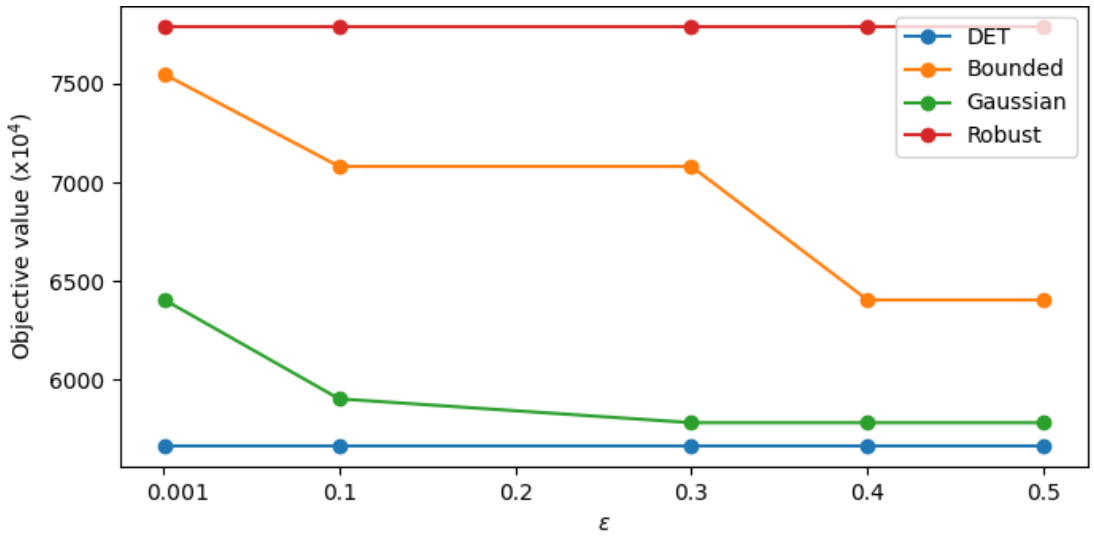

Figure 5.6: Computational results of various models ($\gamma = 0.01$)

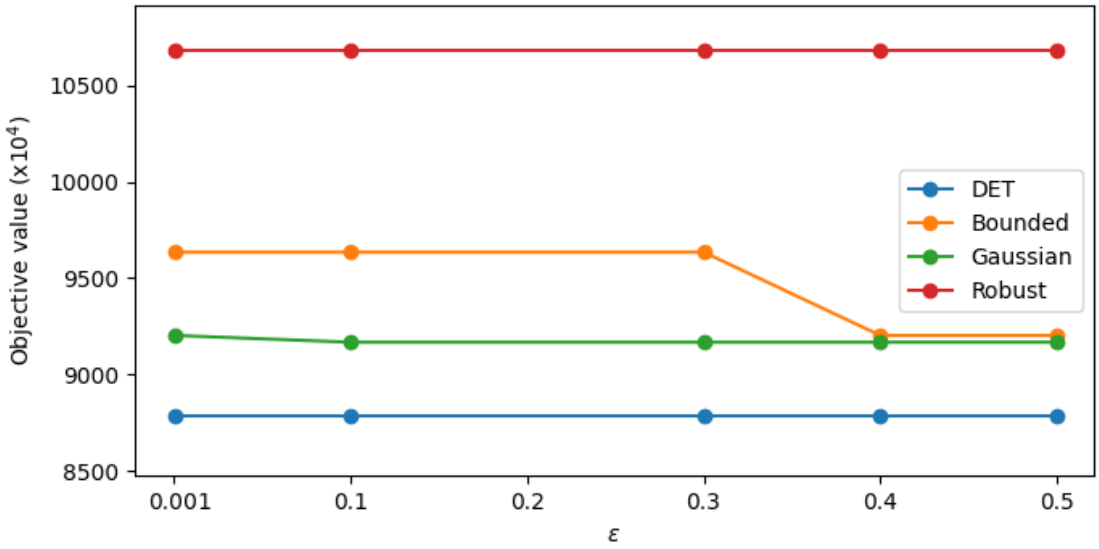

Figure 5.7: Computational results of various models ($\gamma = 0.1$)

under high risk objective focus (high γ), the bounded and Gaussian models converge to the same solution, indicating a threshold beyond which the specific handling of

Table 5.20: Computational results of various models ($\gamma = 0.1$)

ϵ	Model	Cost ($\times 10^4$ RMB)	Risk ($\times 10^5$)	Objective function ($\times 10^4$)	# of facilities
-	DET	6,527.5	2,260	8,788	7
-	Robust	7,727.5	2,956	10,683	9
0.001	Bounded	7,727.5	1,908	9,635	9
	Gaussian	7,127.5	2,075	9,203	8
0.1	Bounded	7,727.5	1,908	9,635	9
	Gaussian	5,727.5	3,440	9,168	6
0.3	Bounded	7,727.5	1,908	9,635	9
	Gaussian	5,727.5	3,440	9,168	6
0.4	Bounded	7,127.5	2,075	9,203	8
	Gaussian	5,727.5	3,440	9,168	6
0.5	Bounded	7,127.5	2,075	9,203	8
	Gaussian	5,727.5	3,440	9,168	6

risk becomes less distinct between the models.

5.2.6.4 System Performance Under Various Uncertain Scenarios

The presence of uncertainties in emergency hazmat network design introduces complexities that traditional deterministic models may overlook. Hence, we concentrate on system risk and conduct a thorough comparative analysis. We compare the performance of our proposed DRO models with the deterministic and robust models to assess the effects of uncertainties on system performance and resilience and shed light on the effectiveness of the different modeling approaches in addressing these

Table 5.21: Computational results of various models ($\gamma = 1$)

ϵ	Model	Cost ($\times 10^4$ RMB)	Risk ($\times 10^5$)	Objective function ($\times 10^4$)	# of facilities
-	DET	9,727.5	1,447	24,195	12
-	Robust	9,727.5	2,315	32,875	12
0.001 - 0.5	Bounded	9,727.5	1,500	24,723	12
	Gaussian	9,727.5	1,500	24,723	12
0.1	Bounded	9,727.5	1,500	24,723	12
	Gaussian	9,727.5	1,500	24,723	12
0.3	Bounded	9,727.5	1,500	24,723	12
	Gaussian	9,727.5	1,500	24,723	12
0.4	Bounded	9,727.5	1,500	24,723	12
	Gaussian	9,727.5	1,500	24,723	12
0.5	Bounded	9,727.5	1,500	24,723	12
	Gaussian	9,727.5	1,500	24,723	12

challenges. To evaluate the models under real-world conditions, we use $\epsilon = 0.1$ and construct 5 uncertainty scenarios from our original response time data to reflect possible uncertain situations within the network.

The first scenario (U01) simulates a moderate a 10% increase in travel time, reflecting slightly adverse conditions. The second scenario (U02) simulates a 50% delay in travel time, indicating significant delays in the transportation network during peak hours. Scenario U03 illustrates a doubling of travel time, indicating disruptions such as major road closures or accidents. The fourth scenario (U04) represents an extreme scenario with triple the average travel time, indicating more severe disruptions. We

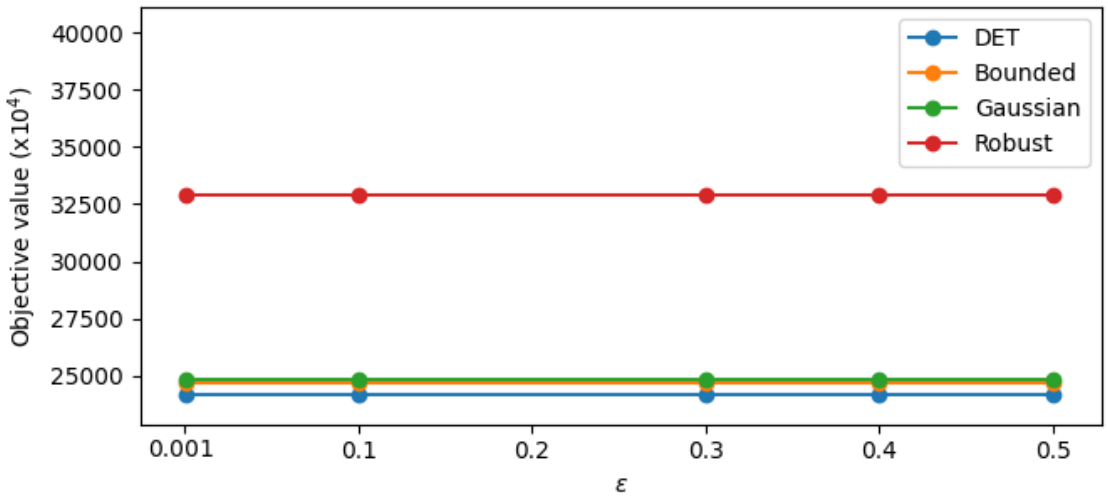

Figure 5.8: Computational results of various models ($\gamma = 1$)

employ scenario U05 with five times the usual travel time as the worst-case scenario to represent severe disruptions such as natural disasters or extreme weather events.

Consequently, the four distinct system designs: Deterministic, Robust, Bounded, and Gaussian models, undergo analysis under these uncertainty scenarios. The test demonstrates how different systems constructed using various models respond to the various uncertainty situations to provide emergency services effectively. At this stage, the facilities are fixed and we test our models to minimize risk in the event of the uncertainty. To account for the unplanned uncertainties which have the potential to overly violate the system requirements, we modify the model as follows.

$$\min \sum_{i\in\mathcal{I}} \sum_{j\in\mathcal{J}} \sum_{k\in\mathcal{K}} T_{ij}E_{jk}x_{ijk} + (T_{ij} - \theta)^{+}E_{\max}x_{ijk}$$

s.t.

$$\sum_{i\in\mathcal{I}} x_{ijk} \geq W_{jk}, \qquad \forall j \in \mathcal{J}, \forall k \in \mathcal{K}$$

$$\sum_{j\in\mathcal{J}} x_{ijk} \leq q_{ik}, \qquad \forall i \in \mathcal{I}, \forall k \in \mathcal{K}$$

$$x_{ijk} \geq 0, \quad \text{integer}, \qquad \forall i \in \mathcal{I}, \forall j \in \mathcal{J}, \forall k \in \mathcal{K}$$

where $E_{\max} = \max E_{jk}$ represents the maximum risk associated with all response times exceeding θ $(T_{ij} - \theta)$ over all incident sites to reflect the resulting high risk, with

$$(T_{ij} - \theta)^+ = \begin{cases} T_{ij} - \theta, & \text{if } T_{ij} - \theta > 0 \\ 0, & \text{if } T_{ij} - \theta \leq 0. \end{cases}$$

The results provided in Figure 5.9 offer compelling insights into the comparative risks associated with each model across varying uncertainty scenarios. Notably, while the deterministic model demonstrates efficiency when there is certainty in the network, it becomes highly vulnerable to risk escalation as uncertainties are introduced, making it less suitable for handling real-world uncertainties. On the other hand, the risk in the RO model remains the lowest irrespective of the uncertainty scenarios outlined in this analysis. However, the RO model typically incurs the highest costs compared to the other models under study for system design, leading to an overestimation of risks in anticipation of worst-case scenarios. Specifically, the RO model

incurs approximately 39.01% more cost than the deterministic model. The DRO models take into account the uncertainty distribution and aim to optimize solutions that are robust against variations within the distribution while maintaining optimal cost. Both the Bounded and Gaussian models demonstrate noteworthy capabilities in mitigating risk. With uncertainties, the DRO models generally lag behind the RO model in terms of risk performance as the uncertainty increases, but they perform better in cost management by not over-preparing for uncertainties. Specifically, the Bounded model produces 8.42% better cost efficiency than the RO model while delivering risk mitigation that is 7.3% behind the RO model. The Gaussian model also achieves excellent cost efficiency compared to the RO model, even though its risk mitigation output lags behind the RO model. Generally, both DRO models aim to strike a balance between cost and risk objectives, with the Bounded model placing more emphasis on risk minimization and the Gaussian model concentrating more on cost optimization. Furthermore, we analyzed the average response time (T_{ij}) and the maximum response time across the five different uncertainty scenarios and present the results in Table 5.22. Under the deterministic model, average response times range from 4.20 to 18.15 units, while the DRO and RO models present better values. Comparably, the RO and DRO models demonstrate superior performance, with reduced average response times across all uncertainty scenarios. However, when the cost to design the RO and DRO models are considered, the DRO models appear to have better overall performance. Ultimately, the choice between RO and DRO

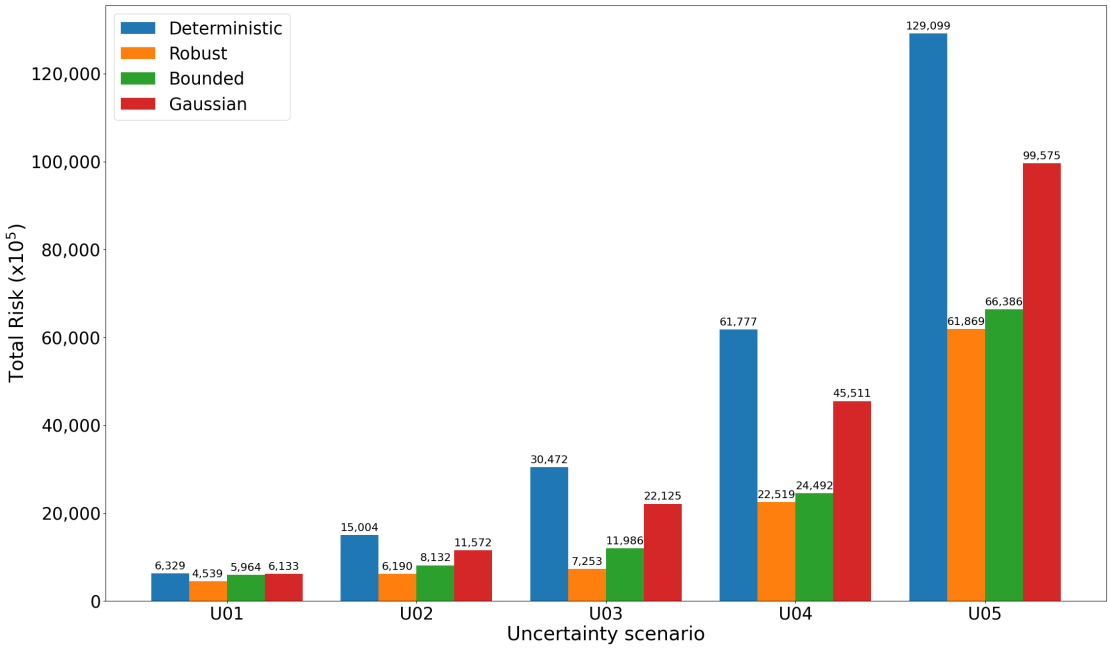

Figure 5.9: Comparison of uncertain risk for different models

hinges on various factors, such as the decision-makers' risk preferences. While the RO model prioritizes robustness under all possible scenarios with a high cost of robustness in its conservative approach, the DRO model offers advantages in overall system performance by balancing robustness and cost-effectiveness.

5.2.6.5 Facility Utilization Across Models

This section analyzes the utilization of facilities constructed under each model and summarized in Table 5.23. With the total allocated emergency units across the network = 371 emergency units for all models, we determine the percentage of unused capacity by finding the ratio of the allocated emergency units to the combined total

Table 5.22: System Performance Under Different Scenarios

Model	Function	U1	U2	U3	U4	U5
DET	Average T_{ij}	4.20	5.44	7.26	10.89	18.15
	Maximum T_{ij}	10.34	13.5	18	27	45
Robust	Average T_{ij}	2.31	3.15	4.20	6.24	10.40
	Maximum T_{ij}	5.5	7.5	10	15	25
Bounded	Average T_{ij}	2.37	3.24	4.32	6.47	10.79
	Maximum T_{ij}	6.38	8.7	11.6	17.4	29
Gaussian	Average T_{ij}	3.45	4.71	6.28	9.72	16.22
	Maximum T_{ij}	8.8	12	16	27	45

capacity of all constructed facilities. Thus, the deterministic model shows high utilization efficiency with only 4.87% unused capacity across its five constructed emergency facilities. However, its vulnerability to risk escalation under uncertainty, as discussed in our previous section, limits its practicality. The RO model maintains the lowest risk across varying uncertainty scenarios but has a significant 31.30% of unused capacity. This high network redundancy, coupled with the highest construction cost, further indicates that the RO model overestimates required capacity while trying to safeguard against worst-case uncertainty scenarios. In contrast, the Bounded model balances resource utilization with 24.29% unused capacity. It achieves better cost efficiency than the RO model while maintaining substantial risk mitigation across all uncertainty scenarios. The Gaussian model exhibits 7.25% unused capacity, indicating precise resource allocation. While its risk mitigation is slightly less effective than

Table 5.23: Facility Utilization Across Models

Model	Total Constructed Capacity	Percentage Unused Capacity
DET	390	4.87%
Robust	540	31.30%
Bounded	490	24.29%
Gaussian	400	7.25%

the Bounded model, it excels in cost management and resource utilization, avoiding over-preparation for extreme cases. Comparing these models in terms of both construction cost, redundant capacity and risk mitigation highlights the benefits of DRO models. The DRO models demonstrate superior system utility by achieving a balance between robustness and cost-effectiveness in managing hazmat emergency logistics, making them more suitable for real-world applications where uncertainty is a significant factor.

5.2.7 Variation in Distributional Ambiguity

In this section, we examine how variations in the ambiguity set parameters can influence the DRO models' outcomes in our previous experiments. To facilitate this analysis, we introduce a parameter denoted as $\Delta = \hat{T}_{ij}/\bar{T}_{ij}$, representing the measure of the normal deviation of the uncertain variable to the expected value, which reflects the level of distributional ambiguity. We conduct experiments by solving both the Bounded and Gaussian models at various values of Δ and showcase the results in Fig. 5.10. Clearly, the objective value of the Bounded model increases by over 33.60%

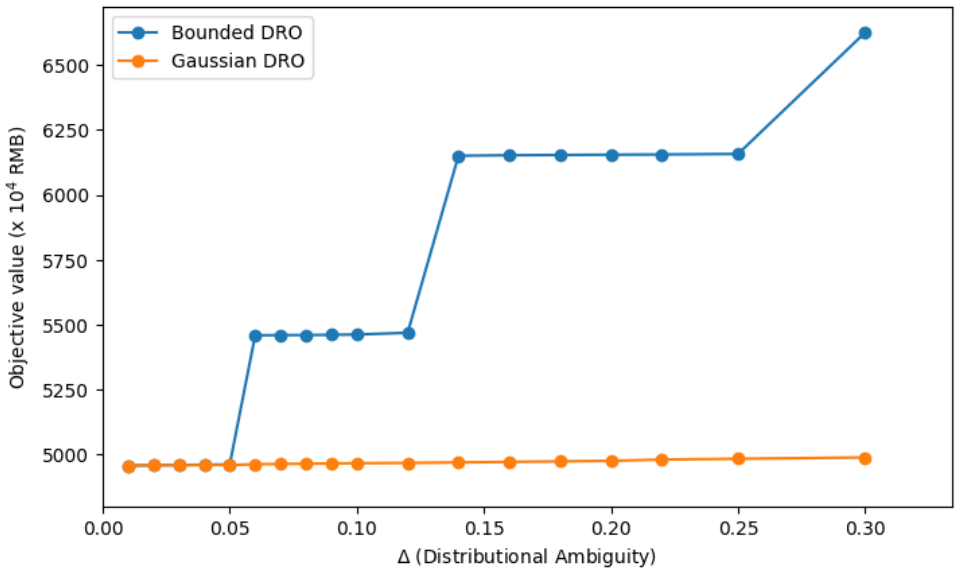

Figure 5.10: Variation in distributional ambiguity

from 4,958 $\times 10^4$ RMB to 6,624 $\times 10^4$ RMB. On the other hand, the Gaussian model demonstrates a more stable pattern across different levels of distributional ambiguity, with only a small increase of 0.63% in the objective value from 4,958 $\times 10^4$ RMB to 4,989 $\times 10^4$ RMB as Δ increases.

To further understand the model behaviors, we separately analyze the impact of Δ on cost and risk, and present them in Fig. 5.11 and Fig. 5.12. For the Bounded model, the number of facilities constructed increases as the distributional ambiguity parameter rises. Specifically, low values of Δ (from 0.01 to 0.05) result in high risk levels, with the risk ranging from 5,576 $\times 10^5$ to 5,620 $\times 10^5$. To keep the construction costs low at 4,400 $\times 10^4$ RMB, only 6 facilities are built. However, the high risk indicates that this minimal investment in facilities is insufficient for effective risk

mitigation. As Δ increases from 0.06 to 0.1, the focus shifts towards reducing risk more effectively. The number of facilities increases to 7, resulting in a noticeable reduction in risk, with values dropping to approximately 4,589 to 4,620 $\times 10^5$. This improved risk management comes at an increased cost of 5,000 $\times 10^4$ RMB, demonstrating a trade-off where higher investment in facilities leads to lower risk. As Δ ranges from 0.12 to 0.25, further investments are made to reduce risk. The number of facilities increases to 8, leading to construction costs rising to 5,600 $\times 10^4$ RMB. Initially, risk decreases but then starts to increase again, peaking at 5,567 $\times 10^5$ for $\Delta = 0.25$. At $\Delta = 0.3$, a conservative effort is made to mitigate risk by constructing 9 facilities. This results in a significant reduction in risk to 4,235 $\times 10^5$, with the highest construction cost of 6,200 $\times 10^4$ RMB$\times 10^4$ RMB. This phase suggests that substantial risk mitigation can be achieved with additional facilities, although at a higher cost.

For the Gaussian model, the values of Δ from 0.01 result in relatively high-risk levels, with the risk starting at 5,576 $\times 10^5$. To keep the construction costs low at 4,400 $\times 10^4$ RMB, only 6 facilities are built. as Δ ranges from 0.01 to 0.3, the risk increases gradually, peaking at 5,889 $\times 10^5$. The number of facilities and the construction cost remain unchanged at 6 and 4,400 $\times 10^4$ RMB, respectively. This phase demonstrates that the Gaussian model maintains the cost efficiency, but the increasing Δ values lead to higher risk levels, underscoring the distinct behavior of both models in risk management.

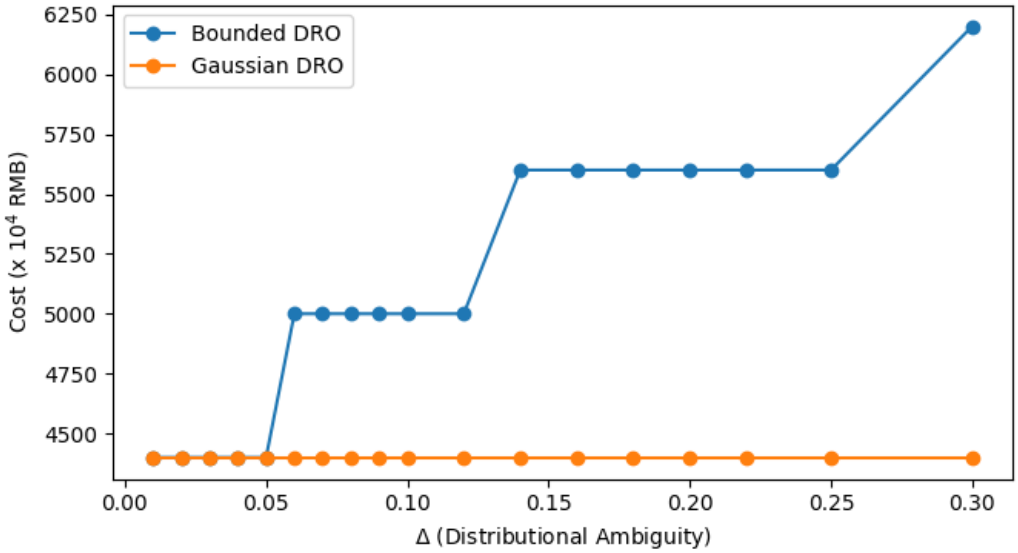

Figure 5.11: Variation in distributional ambiguity - Cost

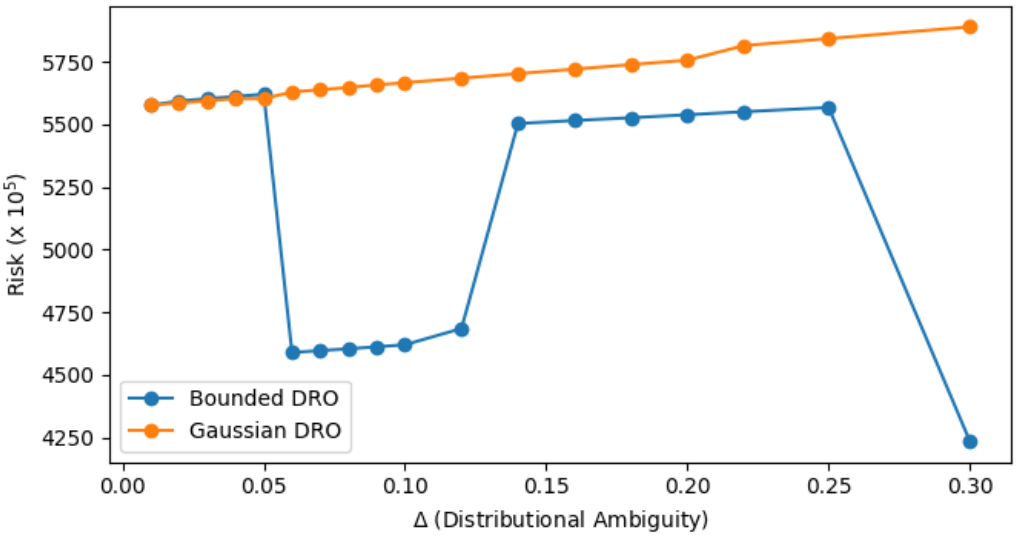

Figure 5.12: Variation in distributional ambiguity - Risk

These findings suggest that the Bounded model exhibits more sensitivity as the distributional ambiguity parameter Δ increases, particularly towards risk mitigation.

This indicates that as uncertainty in the parameters changes, the Bounded model tends to be more conservative, constructing more facilities to manage the increased ambiguity and mitigate risk. In contrast, the Gaussian model demonstrates smaller changes across different levels of distributional ambiguity, which is consistent with previous studies such as Wang et al. (2022). This resilience can be attributed to the Gaussian model's incorporation of a more extensive range of distributional information into the ambiguity sets, equipping it with the capability to withstand changes without substantial impact on its performance.

Chapter 6

Summary and Conclusions

6.1 Overview

This thesis focuses on the intricate challenges of hazmat emergency facility location problems, specifically dealing with optimizing facility location and allocation to enhance preparedness and emergency response. The central objective involves a dual approach: minimizing costs and timely mitigating risks. The proposed solution is a Distributionally Robust Optimization (DRO) chance-constrained model that considers uncertainty in emergency response times. This DRO model addresses multiple facets simultaneously, determining facility locations, constructions, hazardous response unit placement, and emergency response unit allocation. Its overarching goal is to minimize overall system risk associated with hazmat emergency response and the associated construction/maintenance costs. Moreover, the increased avail-

ability of emergency facilities is identified as a practical means of reducing overall risk. A notable aspect in our thesis is the model's capability to overcome limitations of conventional robust optimization by incorporating partial probability distribution information, avoiding overly conservative solutions. This approach effectively handles uncertainty related to probability distribution, a consideration often overlooked in stochastic optimization models with fixed probability distribution.

Two distinct ambiguity sets are introduced for the chance constraints, each resolved into computable forms for exact optimal solutions. The first set deals with distributions featuring bounded perturbations and zero mean, employing a safe tractable approximation method. The second set involves Gaussian distributions with partial knowledge of expectations and variances, addressed through an equivalent mixed-integer second-order cone programming formulation. Both models demonstrate short solution times, making them suitable for larger networks and presenting valuable approaches for hazmat emergency response optimization, each with unique advantages.

Practical computations are presented, focusing on solving hazmat emergency facility location problems to ensure a timely and effective response to hazmat incidents. The models' effectiveness is demonstrated through a hypothetical problem and a real-world case study in Daojiao, China, showcasing their ability to handle complex network configurations, uncertainties, and varying optimization objectives when partial distribution information on uncertain response times is available. The comparison between the Bounded and Gaussian models highlights distinct strengths

and trade-offs, providing decision-makers with versatile tools for optimizing hazmat emergency response strategies based on specific contextual needs and optimization objectives. Insights from the Bounded model reveal sensitivity to tolerance levels, leading to different outcomes in facility costs, risk, and the number of constructed facilities. As tolerance increases, reduced cost efficiency and risk management become apparent, emphasizing the delicate balance between confidence in response time and facility optimization. Additionally, a notable relationship surfaces between cost and risk, indicating that stringent tolerance requirements may prioritize risk reduction, potentially resulting in escalated facility construction costs. Similarly, the Gaussian model exhibits sensitivity to tolerance levels, showing improved outcomes with relaxation of the tolerance. Its flexibility in managing uncertainties results in better cost solutions as tolerance levels increase. The model's response to uncertainty is characterized by a trade-off between robustness and cost management, strategically positioning additional facilities to enhance system resilience with increasing Gaussian variances (σ). Comparisons under different risk coefficient values consistently illustrate the Gaussian model's out-performance at lower risk coefficients, showcasing its effectiveness in balancing cost and risk objectives. The computational results overall establish the superiority of DRO models, particularly the Gaussian model, with comparative analyses against classical RO models supporting claims regarding solution quality and optimal facility locations. In summary, while the Bounded model excels in handling the risk objective with greater efficiency, the Gaussian model demon-

strates superior cost management capabilities, offering a comprehensive perspective on hazmat emergency response optimization.

6.2 Managerial Insights

Drawing from the thesis, the following managerial insights emerge.

In reality, when designing hazmat emergency networks, obtaining precise distribution information on uncertain response times through historical data is challenging due to various unpredictable factors. Relying on the optimal decision of the deterministic and robust models can lead to significant losses and is therefore not advisable. In such scenarios, decision-makers can consider utilizing the hazmat emergency DRO models proposed in this study. Hence, if the distribution information for uncertain response time for an emergency response network falls within the ambiguity set with bounded perturbations having zero means, decision-makers may opt for the Bounded DRO model. Otherwise, if the distribution information aligns with Gaussian perturbations characterized by partial knowledge of expectations and variances, decision-makers may prefer the Gaussian DRO model.

From the thesis, we see the critical influence of tolerance level on optimal solutions, serving as a key indicator of decision-makers' risk preferences. This insight prompts the recommendation for decision-makers to meticulously choose tolerance levels aligned with their risk attitudes. Striking a strategic balance between response time confidence and facility optimization emerges as a crucial factor for effective haz-

mat emergency response.

The research reveals that the Bounded model demonstrates higher sensitivity to tolerance levels, affecting outcomes in facility costs, risk, and the number of constructed facilities. This insight advises decision-makers to conduct a thorough evaluation of the trade-off between tolerance levels and their impact on cost efficiency and risk management. Strategic assessment is recommended to determine the optimal number of facilities necessary for effective hazmat emergency response based on decision-makers' risk tolerance.

The Gaussian model's flexibility in managing cost and risk objectives, leading to improved solutions with various tolerance levels is a noteworthy insight. Decision-makers can leverage this flexibility by adapting a tolerance level based on the trade-off between robustness and cost management. Such adaptability proves valuable in diverse hazmat scenarios where uncertainties vary. Thus, the superior performance of the Gaussian model can be harnessed to create comprehensive hazmat emergency response strategies in an integrated decision framework to effectively balance both cost and risk objectives.

Finally, it is imperative to account for uncertainties in emergency logistics planning. Estimating or predicting response times during hazmat emergency incidents can be challenging due to various travel conditions and transportation delays. In such case, the DRO model provides a reliable solution for long-term decisions, like determining the location and capacity of emergency facilities, while accommodating

short-term allocation adjustments amidst uncertainties. The selection between RO and DRO must be made based on a thorough analysis of the decision-makers' risk preferences. While the RO model ensures robustness under all scenarios with a very conservative approach, both the Bounded and Gaussian DRO models showcased in this study exhibit significant risk mitigation capabilities, enhancing overall system performance while offering a cost-effective approach for hazmat emergency logistics.

6.3 Future Plans

It is important to note that our research is in its initial and exploratory stage with regard to studying uncertain response times in hazmat emergency facility location problems. Future work should involve considering a more intricate background in this field and incorporating additional factors into the model to better reflect the real-world situation of hazmat emergency management. For instance, if emergency facilities are constructed pre-disaster, ensuring the emergency system's performance post-disaster will be crucial, requiring a two-stage modeling approach. Also, the establishment of an efficient emergency logistics system may require collaboration from various entities, including government authorities and response management. Future works can utilize game theory to explore the dynamics and potential conflicts arising from the interactions among these stakeholders in this setting.

Additionally, while assuming random response times in our study to reflect real-world circumstances, we acknowledge that uncertainties may arise from other param-

eters such as demand and cost due to various factors. Future research could address the incorporation of multiple uncertain parameters for more realistic industry applications.

Lastly, while the current models successfully solve the tested problem cases with minimal computational time, the complexity from much larger problem instances may incur substantial computation times. Therefore, there is a need to design and test an efficient algorithm to handle larger-scale problems.

Bibliography

Foad Akbari, Jaber Valizadeh, and Ashkan Hafezalkotob. Robust cooperative planning of relief logistics operations under demand uncertainty: A case study on a possible earthquake in Tehran. *International Journal of Systems Science: Operations & Logistics*, 9(3):405–428, July 2022. ISSN 2330-2674. doi: 10.1080/23302674.2021.1914767.

Abolfazl Aliakbari, Alireza Rashidi Komijan, Reza Tavakkoli-Moghaddam, and Esmaeil Najafi. A new robust optimization model for relief logistics planning under uncertainty: A real-case study. *Soft Computing*, 26(8):3883–3901, April 2022. ISSN 1433-7479. doi: 10.1007/s00500-022-06823-4.

Shi An, Na Cui, Yun Bai, Weijun Xie, Mingliu Chen, and Yanfeng Ouyang. Reliable emergency service facility location under facility disruption, en-route congestion and in-facility queuing. *Transportation Research Part E: Logistics and Transportation Review*, 82:199–216, October 2015. ISSN 13665545. doi: 10.1016/j.tre.2015.07.006.

Ehsan Ardjmand, Gary Weckman, Namkyu Park, Pooya Taherkhani, and Manjeet Singh. Applying genetic algorithm to a new location and routing model of hazardous materials. *International Journal of Production Research*, 53(3):916–928, February 2015. ISSN 0020-7543. doi: 10.1080/00207543.2014.942010.

Mostafa Bababeik, Navid Khademi, and Anthony Chen. Increasing the resilience level of a vulnerable rail network: The strategy of location and allocation of emergency relief trains. *Transportation Research Part E: Logistics and Transportation Review*, 119:110–128, November 2018. ISSN 1366-5545. doi: 10.1016/j.tre.2018.09.009.

Opher Baron, Joseph Milner, and Hussein Naseraldin. Facility Location: A Robust Optimization Approach. *Production and Operations Management*, 20(5): 772–785, September 2011. ISSN 1059-1478, 1937-5956. doi: 10.1111/j.1937-5956.2010.01194.x.

Aharon Ben-Tal and Arkadi Nemirovski. Robust solutions of Linear Programming problems contaminated with uncertain data. *Mathematical Programming*, 88(3): 411–424, September 2000. ISSN 0025-5610. doi: 10.1007/PL00011380.

Aharon Ben-Tal, Laurent El Ghaoui, and Arkadi Nemirovski. *Robust Optimization*, volume 28. Princeton university press, 2009.

Paul G. Berglund and Changhyun Kwon. Robust Facility Location Problem for

Hazardous Waste Transportation. *Networks and Spatial Economics*, 14(1):91–116, March 2014. ISSN 1572-9427. doi: 10.1007/s11067-013-9208-4.

Oded Berman, Vedat Verter, and Bahar Y. Kara. Designing emergency response networks for hazardous materials transportation. *Computers & Operations Research*, 34(5):1374–1388, May 2007. ISSN 0305-0548. doi: 10.1016/j.cor.2005.06.006.

Board. *A Guide for Assessing Community Emergency Response Needs and Capabilities for Hazardous Materials Releases*. Transportation Research Board, 2011.

Justin J. Boutilier and Timothy C. Y. Chan. Ambulance Emergency Response Optimization in Developing Countries. *Operations Research*, 68(5):1315–1334, September 2020. ISSN 0030-364X. doi: 10.1287/opre.2019.1969.

Kuo-Hao Chang, Yi-Chieh Chiang, and Tzu-Yin Chang. Simultaneous location and vehicle fleet sizing of relief goods distribution centers and vehicle routing for post-disaster logistics. *Computers & Operations Research*, 161:106404, January 2024. ISSN 03050548. doi: 10.1016/j.cor.2023.106404.

Chinese National Registered Architect Management Committee. *Architect Technical Economy and Management (Trial Edition)*. Datu Xu, 1995.

Adel Pourghader Chobar, Majid Sabk Ara, Samaneh Moradi Pirbalouti, Mehdi Khadem, and Saeed Bahrami. A Multi-Objective Location-Routing Problem Model for Multi- Device Relief Logistics under Uncertainty Using Meta-Heuristic Algorithm. *Journal of Applied Research on Industrial Engineering*, 9:354–373, 2022.

Liz Cookman. What caused the Beirut explosion? Everything we know so far. https://www.thenationalnews.com/world/mena/what-caused-the-beirut-explosion-everything-we-know-so-far-1.1059236, August 2020.

Qian Dai and Jiaqi Yang. A Distributionally Robust Chance-Constrained Approach for Modeling Demand Uncertainty in Green Port-Hinterland Transportation Network Optimization. *Symmetry*, 12(9):1492, September 2020. ISSN 2073-8994. doi: 10.3390/sym12091492.

Erick Delage and Yinyu Ye. Distributionally Robust Optimization Under Moment Uncertainty with Application to Data-Driven Problems. *Operations Research*, 58 (3):595–612, June 2010. ISSN 0030-364X, 1526-5463. doi: 10.1287/opre.1090.0741.

Zhiming Ding, Xinrun Xu, Shan Jiang, Jin Yan, and Yanbo Han. Emergency logistics scheduling with multiple supply-demand points based on grey interval. *Journal of Safety Science and Resilience*, 3(2):179–188, June 2022. ISSN 26664496. doi: 10.1016/j.jnlssr.2022.01.001.

Jianhui Du, Peng Wu, Yiqing Wang, and Dan Yang. Multi-stage humanitarian emergency logistics: Robust decisions in uncertain environment. *Natural Hazards*, 115(1):899–922, January 2023. ISSN 1573-0840. doi: 10.1007/s11069-022-05578-3.

Okan Dukkanci, Achim Koberstein, and Bahar Y. Kara. Drones for relief logistics under uncertainty after an earthquake. *European Journal of Operational Research*, 310(1):117–132, October 2023. ISSN 0377-2217. doi: 10.1016/j.ejor.2023.02.038.

E. Ehsan, A. Makui, and K. Shahanaghi. Emergency response network design for hazardous materials transportation with uncertain demand. *International Journal of Industrial Engineering Computations*, 3(5):893–906, 2012.

A. A. Eshghi, R. Tavakkoli-Moghaddam, S. Ebrahimnejad, and V. R. Ghezavati. Multi-objective robust mathematical modeling of emergency relief in disaster under uncertainty. *Scientia Iranica*, 29(5):2670–2695, October 2022. ISSN 1026-3098. doi: 10.24200/sci.2020.54485.3770.

Xuehong Gao and Cejun Cao. Multi-commodity rebalancing and transportation planning considering traffic congestion and uncertainties in disaster response. *Computers & Industrial Engineering*, 149:106782, November 2020. ISSN 03608352. doi: 10.1016/j.cie.2020.106782.

Zabih Ghelichi, Monica Gentili, and Pitu B. Mirchandani. Drone logistics for uncertain demand of disaster-impacted populations. *Transportation Research Part C: Emerging Technologies*, 141:103735, August 2022. ISSN 0968-090X. doi: 10.1016/j.trc.2022.103735.

Ghada Hamouda, Frank Saccomanno, and Liping Fu. Quantitative Risk Assessment Decision-Support Model for Locating Hazardous Materials Teams. *Transportation Research Record: Journal of the Transportation Research Board*, 1873(1):1–8, January 2004. ISSN 0361-1981, 2169-4052. doi: 10.3141/1873-01.

Zhao Jiahong and Shuai Bin. A new multi-objective model of location-allocation

in emergency response network design for hazardous materials transportation. In *2010 IEEE International Conference on Emergency Management and Management Sciences*, pages 246–249, August 2010. doi: 10.1109/ICEMMS.2010.5563457.

Ginger Y. Ke. Managing reliable emergency logistics for hazardous materials: A two-stage robust optimization approach. *Computers & Operations Research*, 138: 105557, February 2022. ISSN 03050548. doi: 10.1016/j.cor.2021.105557.

Ginger Y. Ke and James H. Bookbinder. Emergency Logistics Management for Hazardous Materials with Demand Uncertainty and Link Unavailability. *Journal of Systems Science and Systems Engineering*, 32(2):175–205, April 2023. ISSN 1004-3756, 1861-9576. doi: 10.1007/s11518-023-5554-z.

Ginger Y. Ke, Saeed Shakeri Nezhad, and David M. Tulett. Regulating hazardous material transportation: A scenario-based network design approach with integrated risk-mitigation mechanisms. *International Journal of General Systems*, 53(2):184–214, February 2024. ISSN 0308-1079. doi: 10.1080/03081079.2023.2269469.

Esra Koca, Nilay Noyan, and Hande Yaman. Two-stage facility location problems with restricted recourse. *IISE Transactions*, 53(12):1369–1381, December 2021. ISSN 2472-5854. doi: 10.1080/24725854.2021.1910883.

Tanmoy Kundu, Jiuh-Biing Sheu, and Hsin-Tsz Kuo. Emergency logistics management—Review and propositions for future research. *Transportation Re-*

search Part E: Logistics and Transportation Review, 164:102789, August 2022. ISSN 1366-5545. doi: 10.1016/j.tre.2022.102789.

Hui Li, Jin Peng, Shengguo Li, and Chuang Su. Dispatching medical supplies in emergency events via uncertain programming. *Journal of Intelligent Manufacturing*, 28(3):549–558, March 2017. ISSN 1572-8145. doi: 10.1007/s10845-014-1008-2.

Qirong Li. Study on emergency logistics location-route problem under uncertain demand. In *Second International Conference on Algorithms, Microchips, and Network Applications (AMNA 2023)*, volume 12635, pages 122–127. SPIE, May 2023. doi: 10.1117/12.2679063.

Xueping Li, Zhaoxia Zhao, Xiaoyan Zhu, and Tami Wyatt. Covering models and optimization techniques for emergency response facility location and planning: A review. *Mathematical Methods of Operations Research*, 74(3):281–310, December 2011. ISSN 1432-2994, 1432-5217. doi: 10.1007/s00186-011-0363-4.

George F. List. Siting Emergency Response Teams: Tradeoffs Among Response Time, Risk, Risk Equity and Cost. In Leon N. Moses and Dan Lindstrom, editors, *Transportation of Hazardous Materials*, pages 117–133. Springer US, Boston, MA, 1993. ISBN 978-1-4613-6415-3 978-1-4615-3222-4. doi: 10.1007/978-1-4615-3222-4_9.

G.F. List and M.A. Turnquist. Routing and emergency-response-team siting for

high-level radioactive waste shipments. *IEEE Transactions on Engineering Management*, 45(2):141–152, May 1998. ISSN 1558-0040. doi: 10.1109/17.669759.

Kanglin Liu, Qiaofeng Li, and Zhi-Hai Zhang. Distributionally robust optimization of an emergency medical service station location and sizing problem with joint chance constraints. *Transportation Research Part B: Methodological*, 119:79–101, January 2019a. ISSN 01912615. doi: 10.1016/j.trb.2018.11.012.

Yang Liu, Na Cui, and Jianghua Zhang. Integrated temporary facility location and casualty allocation planning for post-disaster humanitarian medical service. *Transportation Research Part E: Logistics and Transportation Review*, 128:1–16, August 2019b. ISSN 13665545. doi: 10.1016/j.tre.2019.05.008.

Jinke Ming, Jean-Philippe P. Richard, Rongshui Qin, and Jiping Zhu. Distributionally robust optimization for fire station location under uncertainties. *Scientific Reports*, 12(1):5394, March 2022. ISSN 2045-2322. doi: 10.1038/s41598-022-08887-6.

Ministry of Transport of the People's Republic of China. Highway Engineering Estimation Index (JTG 3821-2018). Technical report, 2018.

Nilay Noyan. Risk-averse two-stage stochastic programming with an application to disaster management. *Computers & Operations Research*, 39(3):541–559, March 2012. ISSN 03050548. doi: 10.1016/j.cor.2011.03.017.

NYT. Hazmat Crash in Teutopolis, Ill., Leaves 5 Dead - The New York

Times. https://www.nytimes.com/2023/09/30/us/illinois-truck-crash-ammonia-leak.html, September 2023.

Jomon A. Paul and Xinfang (Jocelyn) Wang. Robust location-allocation network design for earthquake preparedness. *Transportation Research Part B: Methodological*, 119:139–155, January 2019. ISSN 01912615. doi: 10.1016/j.trb.2018.11.009.

Portland Fire and Rescue. *Standard of Emergency Response Coverage*. PF&R Oregon, May 2008.

Logan Rance. Ohio Train Derailment: An Ecological and Human Health Disaster? https://earth.org/ohio-trail-derailment/, February 2023.

Xiangyang Ren and Juan Tan. Location Allocation Collaborative Optimization of Emergency Temporary Distribution Center under Uncertainties. *Mathematical Problems in Engineering*, 2022:e6176756, March 2022. ISSN 1024-123X. doi: 10.1155/2022/6176756.

Sigrid Johansen Rennemo, Kristina Fougner Rø, Lars Magnus Hvattum, and Gregorio Tirado. A three-stage stochastic facility routing model for disaster response planning. *Transportation Research Part E: Logistics and Transportation Review*, 62:116–135, February 2014. ISSN 13665545. doi: 10.1016/j.tre.2013.12.006.

F F Saccomanno and B Allen. Locating Emergency Response Capability for Dangerous Goods Incidents on a Road Network. *Transportation research record*, 1193: 1–9, 1988.

F. Sibel Salman and Eda Yücel. Emergency facility location under random network damage: Insights from the Istanbul case. *Computers & Operations Research*, 62: 266–281, October 2015. ISSN 03050548. doi: 10.1016/j.cor.2014.07.015.

Tomoki Sanada and Aya Ishigaki. Modeling of Inventory Routing Problem with Intermediate Locations in Emergency Logistics Considering Uncertainty of Road Conditions. In Chin-Yin Huang, Rob Dekkers, Shun Fung Chiu, Daniela Popescu, and Luis Quezada, editors, *Intelligent and Transformative Production in Pandemic Times*, Lecture Notes in Production Engineering, pages 41–50, Cham, 2023. Springer International Publishing. ISBN 978-3-031-18641-7. doi: 10.1007/978-3-031-18641-7_5.

Karmel S. Shehadeh and Emily L. Tucker. Stochastic Optimization Models for Location and Inventory Prepositioning of Disaster Relief Supplies, June 2022.

Jia Shu, Wenya Lv, and Qing Na. Humanitarian relief supply network design: Expander graph based approach and a case study of 2013 Flood in Northeast China. *Transportation Research Part E: Logistics and Transportation Review*, 146:102178, February 2021. ISSN 13665545. doi: 10.1016/j.tre.2020.102178.

Hua Sun, Ziyou Gao, W. Y. Szeto, Jiancheng Long, and Fangxia Zhao. A Distributionally Robust Joint Chance Constrained Optimization Model for the Dynamic Network Design Problem under Demand Uncertainty. *Networks and Spatial*

Economics, 14(3-4):409–433, December 2014. ISSN 1566-113X, 1572-9427. doi: 10.1007/s11067-014-9236-8.

Huali Sun, Jiamei Li, Tingsong Wang, and Yaofeng Xue. A novel scenario-based robust bi-objective optimization model for humanitarian logistics network under risk of disruptions. *Transportation Research Part E: Logistics and Transportation Review*, 157:102578, January 2022. ISSN 13665545. doi: 10.1016/j.tre.2021.102578.

Longsheng Sun, Mark H. Karwan, and Changhyun Kwon. Robust Hazmat Network Design Problems Considering Risk Uncertainty. *Transportation Science*, December 2015. doi: 10.1287/trsc.2015.0645.

Masoumeh Taslimi, Rajan Batta, and Changhyun Kwon. A comprehensive modeling framework for hazmat network design, hazmat response team location, and equity of risk. *Computers & Operations Research*, 79:119–130, March 2017. ISSN 03050548. doi: 10.1016/j.cor.2016.10.005.

Ali Vaezi, Jyotirmoy Dalal, and Manish Verma. Designing emergency response network for rail hazmat shipments under uncertainties: Optimization model and case study. *Safety Science*, 141:105332, September 2021. ISSN 0925-7535. doi: 10.1016/j.ssci.2021.105332.

Mengran Wan, Chunming Ye, and Dajiang Peng. Multi-period dynamic multi-objective emergency material distribution model under uncertain demand. *En-*

gineering Applications of Artificial Intelligence, 117:105530, January 2023. ISSN 0952-1976. doi: 10.1016/j.engappai.2022.105530.

Duo Wang, Kai Yang, and Lixing Yang. Risk-averse two-stage distributionally robust optimisation for logistics planning in disaster relief management. *International Journal of Production Research*, 61(2):668–691, January 2023a. ISSN 0020-7543. doi: 10.1080/00207543.2021.2013559.

Jing Wang, Jianping Cai, Xiaohang Yue, and Nallan C. Suresh. Pre-positioning and real-time disaster response operations: Optimization with mobile phone location data. *Transportation Research Part E: Logistics and Transportation Review*, 150: 102344, June 2021a. ISSN 13665545. doi: 10.1016/j.tre.2021.102344.

Wei Wang, Shining Wu, Shuaian Wang, Lu Zhen, and Xiaobo Qu. Emergency facility location problems in logistics: Status and perspectives. *Transportation Research Part E: Logistics and Transportation Review*, 154:102465, October 2021b. ISSN 13665545. doi: 10.1016/j.tre.2021.102465.

Weiqiao Wang, Kai Yang, Lixing Yang, and Ziyou Gao. Tractable approximations for the distributionally robust conditional vertex p -Center problem: Application to the location of high-speed railway emergency rescue stations. *Journal of the Operational Research Society*, 73(3):525–539, March 2022. ISSN 0160-5682, 1476-9360. doi: 10.1080/01605682.2020.1843983.

Yu Wang, Jing Wang, Jialiang Chen, and Kai Liu. Optimal Location of Emergency

Facility Sites for Railway Dangerous Goods Transportation under Uncertain Conditions. *Applied Sciences*, 13(11):6608, January 2023b. ISSN 2076-3417. doi: 10.3390/app13116608.

Dongyang Xia, Jihui Ma, Sh. Sharif Azadeh, and Wenyi Zhang. Data-driven distributionally robust timetabling and dynamic-capacity allocation for automated bus systems with modular vehicles. *Transportation Research Part C: Emerging Technologies*, 155:104314, October 2023. ISSN 0968090X. doi: 10.1016/j.trc.2023.104314.

Chunlin Xin, Qingge Letu, and Yin Bai. Robust Optimization for the Hazardous Materials Transportation Network Design Problem. In Peter Widmayer, Yinfeng Xu, and Binhai Zhu, editors, *Combinatorial Optimization and Applications*, Lecture Notes in Computer Science, pages 373–386, Cham, 2013. Springer International Publishing. ISBN 978-3-319-03780-6. doi: 10.1007/978-3-319-03780-6_33.

Jiuping Xu, Jun Gang, and Xiao Lei. Hazmats Transportation Network Design Model with Emergency Response under Complex Fuzzy Environment. *Mathematical Problems in Engineering*, 2013:e517372, May 2013. ISSN 1024-123X. doi: 10.1155/2013/517372.

Ce Yang, Dong Han, Weiqing Sun, and Kunpeng Tian. Distributionally Robust Model of Energy and Reserve Dispatch Based on Kullback–Leibler Di-

vergence. *Electronics*, 8(12):1454, December 2019. ISSN 2079-9292. doi: 10.3390/electronics8121454.

Fanghao Yin and Yi Zhao. Distributionally robust equilibrious hybrid vehicle routing problem under twofold uncertainty. *Information Sciences*, 609:1239–1255, September 2022. ISSN 00200255. doi: 10.1016/j.ins.2022.07.140.

Fanghao Yin, Yanju Chen, Fengxuan Song, and Yankui Liu. A new distributionally robust P-hub median problem with uncertain carbon emissions and its tractable approximation method. *Applied Mathematical Modelling*, 74:668–693, October 2019. ISSN 0307904X. doi: 10.1016/j.apm.2019.04.056.

Bo Zhang, Jin Peng, and Shengguo Li. Covering location problem of emergency service facilities in an uncertain environment. *Applied Mathematical Modelling*, 51:429–447, November 2017. ISSN 0307-904X. doi: 10.1016/j.apm.2017.06.043.

Guowei Zhang, Ning Jia, Ning Zhu, Long He, and Yossiri Adulyasak. Humanitarian transportation network design via two-stage distributionally robust optimization. *Transportation Research Part B: Methodological*, 176:102805, October 2023a. ISSN 01912615. doi: 10.1016/j.trb.2023.102805.

Jianghua Zhang, Yuchen Li, and Guodong Yu. Emergency relief network design under ambiguous demands: A distributionally robust optimization approach. *Expert Systems with Applications*, 208:118139, December 2022. ISSN 09574174. doi: 10.1016/j.eswa.2022.118139.

Jianghua Zhang, Daniel Zhuoyu Long, and Yuchen Li. A reliable emergency logistics network for COVID-19 considering the uncertain time-varying demands. *Transportation Research Part E: Logistics and Transportation Review*, 172:103087, April 2023b. ISSN 1366-5545. doi: 10.1016/j.tre.2023.103087.

Peiyu Zhang, Yankui Liu, Guoqing Yang, and Guoqing Zhang. A distributionally robust optimization model for designing humanitarian relief network with resource reallocation. *Soft Computing*, 24(4):2749–2767, February 2020. ISSN 1432-7643, 1433-7479. doi: 10.1007/s00500-019-04362-z.

Xinyi Zhang, Peng Wu, Chengbin Chu, and MengChu Zhou. A Distributionally Robust Optimization for Reliability-Based Lane Reservation and Route Design Under Uncertainty. *IEEE Transactions on Intelligent Transportation Systems*, pages 1–16, 2023c. ISSN 1524-9050, 1558-0016. doi: 10.1109/TITS.2023.3300769.

Jiahong Zhao and Ginger Y. Ke. Optimizing Emergency Logistics for the Offsite Hazardous Waste Management. *Journal of Systems Science and Systems Engineering*, 28(6):747–765, December 2019. ISSN 1004-3756, 1861-9576. doi: 10.1007/s11518-019-5429-5.

Pengfei Zhao, Chenghong Gu, Da Huo, Yichen Shen, and Ignacio Hernando-Gil. Two-Stage Distributionally Robust Optimization for Energy Hub Systems. *IEEE Transactions on Industrial Informatics*, 16(5):3460–3469, May 2020. ISSN 1551-3203, 1941-0050. doi: 10.1109/TII.2019.2938444.

Konstantinos G. Zografos and Konstantinos N. Androutsopoulos. A decision support system for integrated hazardous materials routing and emergency response decisions. *Transportation Research Part C: Emerging Technologies*, 16(6):684–703, December 2008. ISSN 0968090X. doi: 10.1016/j.trc.2008.01.004.